Journal Pre-proofs

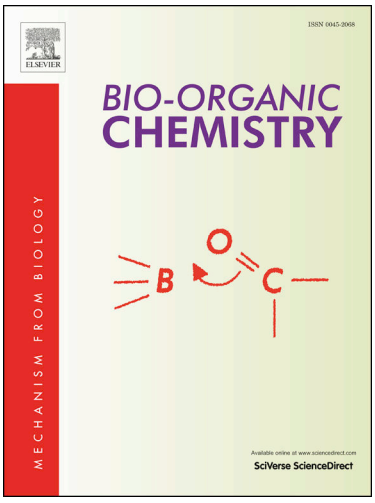

Design and Synthesis of β-carboline linked aryl sulfonyl piperazine derivatives: DNA topoisomerase II inhibition with DNA binding and apoptosis inducing ability

Kesari Lakshmi Manasa, Sowjanya Thatikonda, Dilep Kumar Sigalapalli, Arpita Sagar, Gaddam Kiranmai, Arunasree M Kalle, Mallika Alvala, Chandraiah Godugu, Narayana Nagesh, Bathini Nagendra Babu

PII: S0045-2068(20)31280-3
DOI: https://doi.org/10.1016/j.bioorg.2020.103983
Reference: YBIOO 103983

To appear in: *Bioorganic Chemistry*

Received Date: 9 December 2019
Revised Date: 15 April 2020
Accepted Date: 29 May 2020

Please cite this article as: K. Lakshmi Manasa, S. Thatikonda, D. Kumar Sigalapalli, A. Sagar, G. Kiranmai, A.M. Kalle, M. Alvala, C. Godugu, N. Nagesh, B. Nagendra Babu, Design and Synthesis of β-carboline linked aryl sulfonyl piperazine derivatives: DNA topoisomerase II inhibition with DNA binding and apoptosis inducing ability, *Bioorganic Chemistry* (2020), doi: https://doi.org/10.1016/j.bioorg.2020.103983

Design and Synthesis of *β*-carboline linked aryl sulfonyl piperazine derivatives: DNA topoisomerase II inhibition with DNA binding and apoptosis inducing ability

Kesari Lakshmi Manasa,[a,b] Sowjanya Thatikonda,[c] Dilep Kumar Sigalapalli,[a,b] Arpita Sagar,[e] Gaddam Kiranmai,[d] Arunasree M Kalle,[e] Mallika Alvala,[b] Chandraiah Godugu,[c]* Narayana Nagesh,[d]* and Bathini Nagendra Babu[a]*

[a]*Fluoro-Agrochemicals, CSIR-Indian Institute of Chemical Technology, Hyderabad-500007, India*

[b]*Department of Medicinal Chemistry, National Institute of Pharmaceutical Education and Research (NIPER), Hyderabad-500037, India*

[c]*Department of Regulatory Toxicology, National Institute of Pharmaceutical Education and Research (NIPER), Hyderabad-500037, India*

[d]*CSIR-Centre for Cellular and Molecular Biology, Hyderabad 500 007, India*

[e]*Department of Animal Biology, School of Life Sciences, University of Hyderabad, Hyderabad-500 046, India*

Abstract

A series of new *β*-carboline linked aryl sulfonyl piperazine congeners have been synthesized by coupling various *β*-carboline acids with substituted aryl sulfonyl piperazines. Evaluation of their anticancer activity against a panel of human cancer cell lines such as colon (HT-29), breast (MDA-MB-231), bone osteosarcoma (MG-63), brain (U87 MG), prostate (PC- 3) and normal monkey kidney (Vero) cell line has been done. Among the series, compound **8ec** and **8ed**has shown most potent cytotoxicity with an IC_{50} values of 2.80±0.10 µM and 0.59±0.28 µM respectively against MG-63 cell line and also potent on other cell lines tested. Compounds **8ec** and **8ed**was found to inhibit Topo II that is confirmed by specific Topo II inhibition assay. DNA binding studies, cell cycle analysis, Annexin V study indicate that these compounds has potential anticancer activity. Molecular docking studies for compound **8ec** and **8ed** are incorporated to understand the nature of interaction with topoisomerase IIα and dsDNA.

Keywords: *β*-carboline; Aryl sulfonyl piperazine; Topoisomerase II inhibition; DNA binding studies; Cytotoxicity and Molecular docking.

1. Introduction

In the present scenario, cancer has become a dreadful disease with an increase in the number of patients [1] and an average, 9.6 million deaths are reported in the year 2018 globally and were projected to rise over 13.1 million by 2030 [2]. Cancer is characterized by the uncontrolled proliferation of cells. Most of the chemotherapeutic agents currently in the market target DNA and are highly recommended as the front-line therapies in several cancers. However, they have several limitations such as high toxicity, limited efficacy, non-specificity, poor tolerance, less bioavailability and the development of resistance. Although several targeted therapies are available for few cancers, till date, DNA is still considered as the main target in cancer therapy due to its role in replication and transcription [3]. Therefore there is a need to develop novel compounds targeting the DNA that would induce apoptosis in cancer cells with high specificity.

The *β*-carboline alkaloids contain tricyclic pyrido[3,4-*b*] indole ring system and were naturally obtained from seeds of *Peganum harmala* (*Zygophillaceae*) [4]. These alkaloids are known to exhibit diverse pharmacological properties such as antialzheimer, antiplatelet, anxiolytic, anticonvulsant, antiviral, antimicrobial, anticancer and antiplasmodial properties [5].

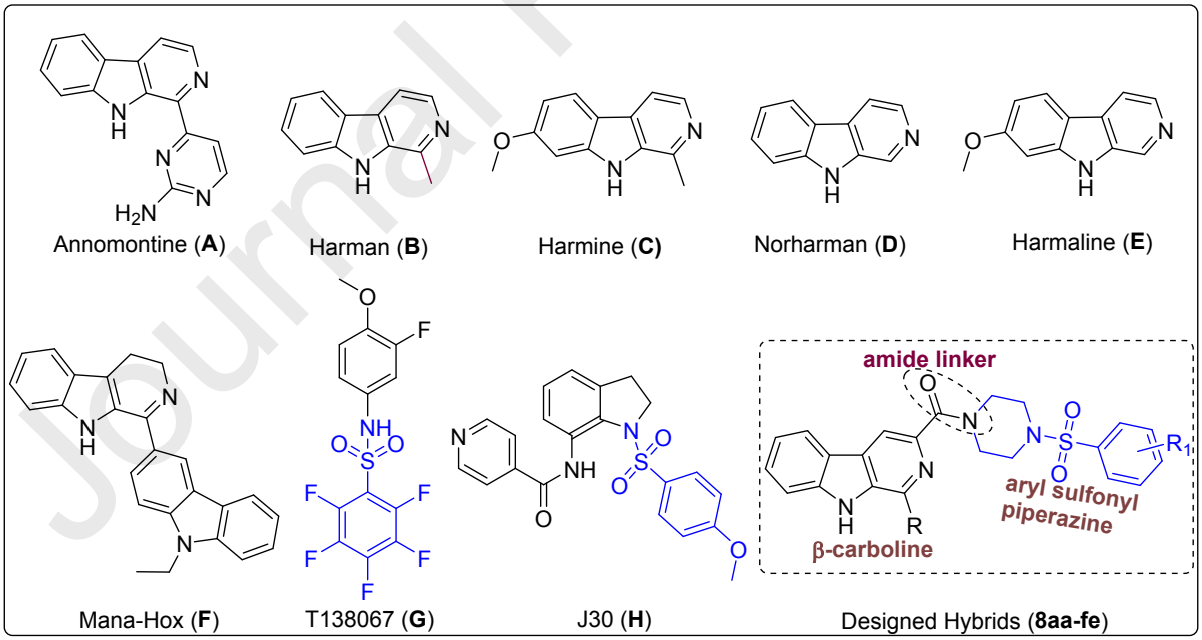

Fig. 1. Structures of biologically active *β*-carbolines (**A**–**F**), sulphonamides (**G** &**H**) and newly designed hybrids (**8aa-fe)**.

β-carboline alkaloids are reported to exhibit anticancer activity *via* multiple mechanisms i.e, DNA intercalation [6], topoisomerase I and II inhibition [7], kinesin Eg5 [8], MK-2 [9] and CDK inhibition [10]. Harmine (**B**), a *β*-carboline analog, possesses DNA intercalation property and inhibits topoisomerase I in various cancer cell lines [11]. Recently Chen *et al* reported a harmine derivative (CM 16) that inhibits the translational step of protein synthesis [12]. Mana-Hox (**C**) is another *β*-carboline analog that intercalates with DNA *via* G-C base pairs [13]. Earlier studies have shown that changes in substitution at C-1 and C-3 positions of *β*-carboline ring exhibit improved DNA binding ability [14].

Sulphonamide congeners are privileged scaffolds having distinct biological activities such as antiviral, antihypertensive, antidiabetic, antithyroid and antibacterial activities [15]. Recently T138067 [16] (**E**, **Fig. 1**) and ABT-751 [17] are novel sulphonamide derivatives came into clinical studies. Moreover, piperazine and its derivatives, with well known heterocyclic scaffold, such as piperazinyl-linked ciprofloxacin dimers [18] are potent antimicrobial agents but also possess antitumor property. AK301 was able to arrest the mitosis and induce the cell apoptosis [19].

Pharmacophore hybridization is an attractive tool for covalently adjoining two distinct biologically important chemical entities into one hybrid molecule [20]. The hybrid molecules with different mechanism of action, might result in synergistic effect with high affinity and selectivity [21].Considering the importance of *β*-carbolines and the biological activity of sulphonamides, our group has put efforts in developing novel *β*-carboline derivatives containing aryl sulfonyl-piperazine scaffold with DNA binding and topoisomerase inhibiting activities aiming the combined substructures may display a synergistic effect on anticancer activity. Herein, we report the design and synthesis of the hybrids of these two pharmacophores with structural diversity by employing simple amidation (**Fig. 2**). Furthermore, the synthesized compounds were evaluated for their cytotoxic activity, cell cycle analysis, DNA binding ability and topoisomerase II inhibitory activity.

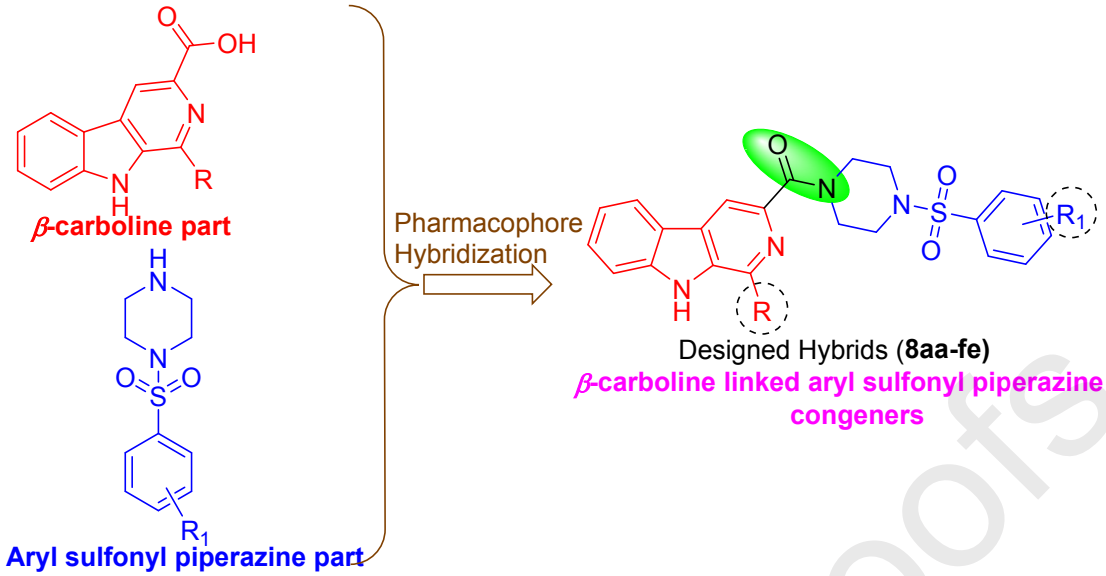

Fig. 2. Pharmacophore Hybridization Strategy for the target molecule.

2. Results and discussion

2.1. Chemistry

The *β*-carboline linked aryl sulfonyl piperazine congeners (**8aa–fe)** were synthesized in a convergent approach by employing the acid amine coupling reaction between substituted *β*-carboline acids (**5a-f**) and substituted phenyl sulfonyl piperazines (**7a-e**) as depicted in **Scheme 1**. The key synthetic precursor L-tryptophan (**1**) was esterified by using $SOCl_2$ in methanol to L-tryptophan methyl ester (**2**), followed by a Pictet-Spengler condensation with variety of substituted benzaldehydes resulted the corresponding methyl tetrahydro-*β*-carboline-3-carboxylates **3a–f.** The diastereomers which are obtained were used directly for the aromatization, using trichloroisocyanuric acid (TCICA) to afford the methyl-*β* carboline-3-carboxylates **4a-f**. These were further hydrolized in the presence of aqueous NaOH solution to get *β*-carboline acids **5a-f** in good yields. Next, a variety of substituted phenyl sulfonyl piperazine intermediates (**7a-e**) were synthesized as to the previous synthetic procedures [15]. Compounds **7a-e** was synthesized by the reaction of different substituted benzene sulfonyl chlorides with piperazine in DCM at 0 ºC for 30 min.

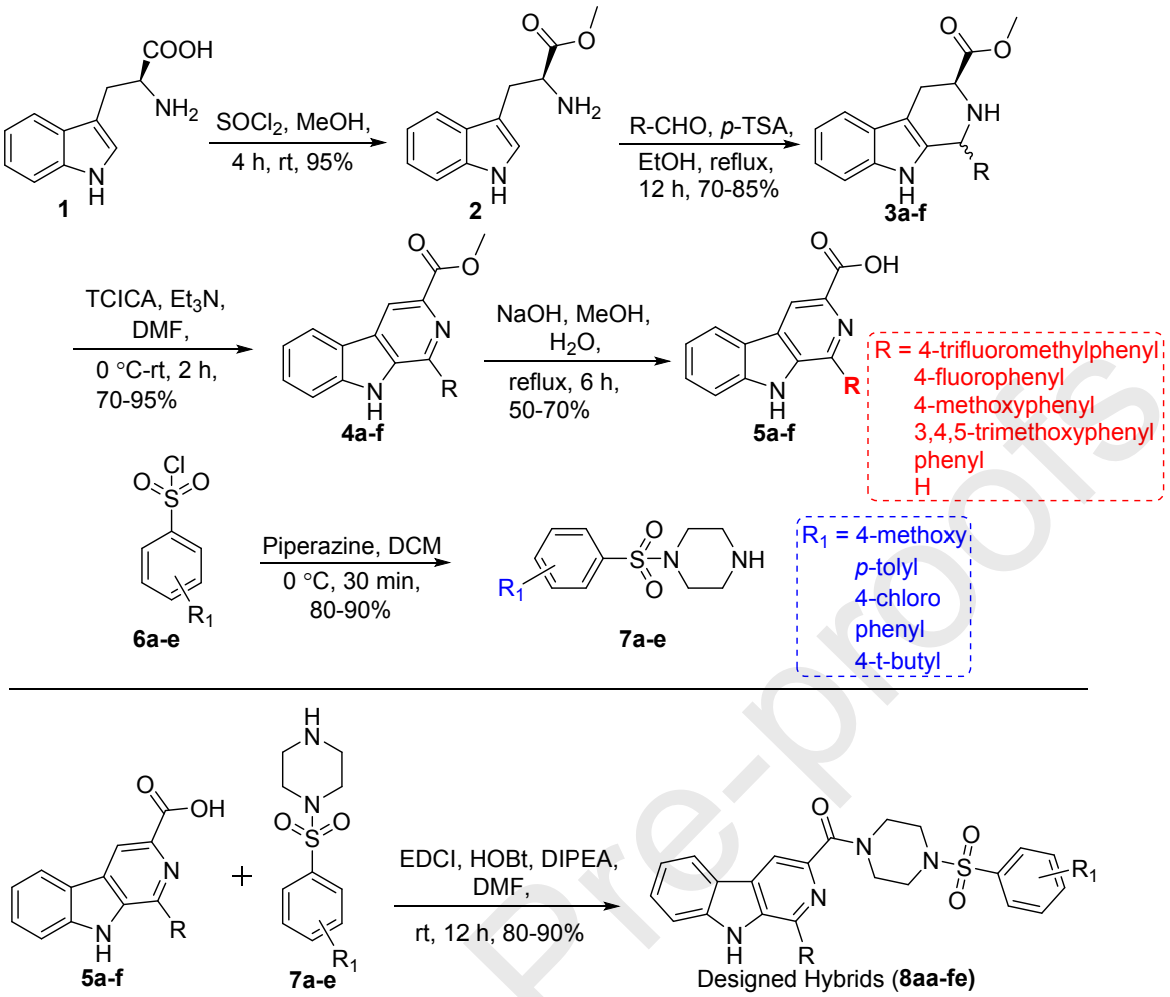

8aa: R = 4-trifluoromethylphenyl, R_1 = 4-methoxy
8ab: R = 4-trifluoromethylphenyl, R_1 = *p*-tolyl
8ac: R = 4-trifluoromethylphenyl, R_1 = 4-chloro
8ad: R = 4-trifluoromethylphenyl, R_1 = phenyl
8ae: R = 4-trifluoromethylphenyl, R_1 = 4-t-butyl
8ba: R = 4-fluorophenyl, R_1 = 4-methoxy
8bb: R = 4-fluorophenyl, R_1 = *p*-tolyl
8bc: R = 4-fluorophenyl, R_1 = 4-chloro
8bd: R = 4-fluorophenyl, R_1 = phenyl
8be: R = 4-fluorophenyl, R_1 = 4-t-butyl
8ca: R = 4-methoxyphenyl, R_1 = 4-methoxy
8cb: R = 4-methoxyphenyl, R_1 = *p*-tolyl
8cc: R = 4-methoxyphenyl, R_1 = 4-chloro
8cd: R = 4-methoxyphenyl, R_1 = phenyl
8ce: R = 4-methoxyphenyl, R_1 = 4-t-butyl
8da: R = 3,4,5-trimethoxyphenyl, R_1 = 4-methoxy
8db: R = 3,4,5-trimethoxyphenyl, R_1 = *p*-tolyl
8dc: R = 3,4,5-trimethoxyphenyl, R_1 = 4-chloro
8dd: R = 3,4,5-trimethoxyphenyl, R_1 = phenyl
8de: R = 3,4,5-trimethoxyphenyl, R_1 = 4-t-butyl
8ea: R = phenyl, R_1 = 4-methoxy
8eb: R = phenyl, R_1 = *p*-tolyl
8ec: R = phenyl,R_1 = 4-chloro
8ed: R = phenyl,R_1 = phenyl
8ee: R = phenyl, R_1 = 4-t-butyl
8fa: R = H, R_1 = 4-methoxy
8fb: R = H, R_1 = *p*-tolyl
8fc: R = H, R_1 = 4-chloro
8fd: R = H, R_1 = phenyl
8fe: R = H, R_1 = 4-t-butyl

Scheme 1. Synthesis of *β*-carboline linked arylsulfonyl piperazine compounds**8aa**–**fe**.

Finally, synthesis of desired *β*-carboline-linked aryl sulfonyl piperazine congeners (**8aa–fe)** have been achieved by reacting intermediate **5a-f** with various substituted phenyl sulfonyl piperazines (**7a-e**) in the presence of EDCI and HOBt in DMF and the yields were in

the range of 80-90%. All the structures of these compounds were characterized by ^{1}H NMR, ^{13}C NMR, mass and HRMS spectral data.

One of the representative compounds **8cc** was confirmed by ^{1}H NMR by the appearance of characteristic signal at *δ*11.73 ppm which accounts for 9*H*-indolic of *β*-carboline and the signal at *δ*3.91 ppm accounts for methoxy group. All the aromatic protons of **8cc**were found in the range of *δ*8.38–7.19 ppm**.** The 2 signals at *δ*3.82 and 3.01 ppm accounts for methylinic protons of piperazine. The interpretation of ^{13}C NMR of compound **8cc**depicts carbonyl signals at *δ*167.6 ppm. All other aromatic carbons of **8cc** appeared in the range of *δ*159.8.5–112.5 ppm and aliphatic methoxy carbon at *δ*55.4 ppm. The ^{1}H and ^{13}C NMR spectra of all newly designed compounds **8aa**–**fe** were found almost in a similar pattern and well matched with the respective aromatic and aliphatic signals of their structure. The HRMS (ESI) of newly designed compounds showed characteristic protonated $[M+H]^{+}$ peak to their corresponding molecular formula.

2.2. Evaluation of Biological activity

2.2.1. *In vitro* cytotoxic activity

All the synthesized compounds were screened initially for the percentage growth inhibition (GI_{50} %) on six human cancer cell lines such as PC-3, MDA-MB-231, U87MG, MG-63, HT-29 and HeLa cell line. Compounds which are able to show the percentage growth inhibition less than 40% known to be inactive compounds and percentage inhibition more than 50% are known to be active. The percentage growth inhibition of the tested compounds was listed in **Table 1**. It is noticeable from the results that all the tested compounds shown moderate to potent growth inhibition. Among the series, compounds **8ec** and **8ed** showed potent growth inhibition.

Table 1 *In vitro* growth inhibitory concentration (GI_{50}[a] %) against human cancer cell lines by MTT assay.

Compound	HT-29[b]	MDA-MB-231[c]	MG-63[d]	U87MG[e]	PC3[f]	HeLa[g]
8aa	25.64±3.2	21.57±1.4	53.19±1.4	59.84±1.5	57.44±1.5	73.33±1.7
8ab	10.97±1.2	3.88±1.1	35.11±1.1	57.61±3.2	25.22±1.25	23.17±1.56
8ac	11.07±1.1	28.97±1.5	41.52±1.8	41.92±3.5	51.51±1.5	46.42±1.4
8ad	6.41±0.89	8.26±0.89	18.11±0.89	48.92±3.7	42.02±1.2	33.20±1.3
8ae	11.02±1.2	15.73±1.1	14.63±1.0	51.71±3.1	25.48±1.6	40.71±1.4
8ba	3.46±0.2	30.50±1.5	47.77±1.2	50.23±3.5	48.02±4.5	40.55±1.23
8bb	8.17±0.3	38.50±1.6	49.02±1.5	42.51±4.5	50.60±1.59	51.95±1.56
8bc	15.87±1.25	30.28±1.23	52.63±1.56	26.43±1.2	52.24±1.56	45.50±1.56
8bd	21.94±1.23	23.73±1.45	12.11±1.32	16.28±1.1	51.17±1.25	55.95±1.58

8be	9.84±0.56	19.71±1.2	27.55±1.28	49.20±1.56	37.57±1.45	29.73±1.26
8ca	9.76±0.23	6.30±0.56	30.77±0.38	32.64±1.25	23.95±1.22	50.18±1.58
8cb	7.00±0.25	15.57±1.2	5.36±0.23	22.17±1.25	47.64±1.45	25.79±1.25
8cc	3.53±0.56	23.14±1.2	47.16±1.4	60.92±1.89	27.60±1.22	50.79±1.56
8cd	1.07±0.56	22.83±0.25	53.30±1.56	66.53±1.25	54.80±1.56	44.70±1.44
8ce	5.30±0.12	38.83±0.38	38.66±1.2	60.00±1.45	51.35±1.89	38.94±1.89
8da	30.43±0.32	32.45±1.32	54.25±0.54	45.05±1.45	52.02±1.56	38.75±1.23
8db	6.02±0.89	10.16±0.89	41.16±1.2	16.74±1.23	49.20±1.89	27.16±1.56
8dc	17.64±0.18	37.07±0.56	60.66±1.2	10.92±0.98	40.13±0.45	25.68±1.36
8dd	25.84±0.25	49.21±0.89	66.36±1.1	7.10±0.23	53.86±1.56	30.52±1.32
8de	24.23±0.27	9.40±0.96	64.33±0.64	26.61±0.25	6.06±0.89	36.98±1.56
8ea	14.46±0.15	37.40±0.36	65.58±0.65	43.43±1.45	58.33±0.58	34.81±1.78
8eb	22.61±0.22	78.33±1.7	76.27±0.76	68.61±0.68	71.46±1.75	44.12±1.45
8ec	44.97±0.14	70.04±1.2	68.88±1.68	66.35±1.23	77.68±1.89	26.34±1.45
8ed	71.25±0.14	55.16±0.89	88.86±1.56	58.23±1.56	47.02±1.23	38.49±1.56
8ee	14.76±0.23	13.33±1.2	55.25±1.56	16.43±1.2	87.02±1.89	45.44±1.58
8fa	39.84±0.39	28.85±0.28	43.13±1.56	42.74±1.0	53.91±1.23	46.24±1.45
8fb	19.97±0.18	25.00±1.25	40.22±1.45	35.00±0.56	35.60±1.56	17.93±1.09
8fc	4.05±0.23	18.35±1.23	57.27±1.56	53.74±1.56	8.08±0.56	27.35±0.25
8fd	29.71±0.29	28.69±1.25	56.72±1.23	59.84±1.23	40.68±1.89	36.34±0.36
8fe	57.20±0.56	18.83±1.2	61.75±1.63	57.61±1.22	37.64±0.38	40.68±0.89

[a]Compound concentration required to decrease cell growth to half that of untreated cells. [b]Human colon cancer, [c]Human breast cancer, [d]Human bone osteosarcoma, [e]Human brain cancer, [f]Human prostate cancer, [g]Human cervical cancer. All the values are expressed as % inhibition in which each treatment was performed in triplicate wells.

The newly synthesized *β*-carboline linked aryl sulfonyl piperazine congeners (**8aa–fe)** were evaluated for their *in vitro* cytotoxic activity against a panel of six human cancer cell lines namely HT-29 (colon cancer), MDA-MB-231 (Breast cancer), MG-63 (bone osteosarcoma), U87MG (brain cancer), PC3 (prostate cancer), HeLa (cervical cancer) and normal monkey kidney (Vero) cell lines by employing the 3-(4,5-dimethylthiazol-2-yl)-2,5-diphenyltetrazolium bromide (MTT) assay. The results from *in vitro* cytotoxic studies revealed that the compounds **8aa–fe** exhibited diverse cytotoxic properties and are depicted in **Table 2**.

Notably, these compounds exhibited good to moderate cytotoxicity in the tested cancer cell lines. From the close analysis of the IC_{50} values, it was observed that compound **8ed** was more significant in inducing cytotoxicity on all the tested cancer cells and found to be most potent against MG-63 (bone osteosarcoma) cancer cell line with an IC_{50} value 0.59±0.28 μM whereas in U87MG cell line the IC_{50} value was 4.20±0.30 μM. Interestingly, the compound **8ec**, **8ed** exhibited least toxicity on normal vero cell line with IC_{50} value 9.95±0.67 μM and 8.41±0.12 μM respectively. This indicates that the compound **8ed** was selective towards the cancer cells rather than normal cell lines tested as outlined in **Table 2**.

While the compound **8ec** also displayed remarkable cytotoxicity against MG-63, PC-3 and U87MG with an IC_{50} value 2.80±0.10, 3.36±0.32 and 3.90±0.20 μM respectively. Among the series of compounds **8aa, 8cc, 8cd, 8ea** and **8eb** also showed considerable cytotoxicity in cancer cell lines. SAR analysis revealed that C-1 position of *β*-carboline ring displayed better cytotoxic activity with phenyl substitution (**8ed, 8ec, 8ea** and **8eb**) rather than the substitutions at various positions in the phenyl ring. Compound **8ed**, with phenyl at C-1 position of *β*-carboline and phenyl sulfonyl piperazine proved to be potent among all the synthesized compounds. With respect to the promising *in vitro* cytotoxicity results (**Table 2**), the significant activity of newly synthesized hybrids **8aa–fe** could also be attributed towards C1 modification of *β*-carboline by H and CH_3 group at this position. Hence the most active compounds (**8ec** and **8ed**) were further explored for their apoptotic induction studies, DNA topoisomerase II inhibition, DNA interaction studies and molecular docking studies.

Table 2 IC_{50}[a] (μM) of different compounds at 48 h post treatment on the HT-29[b], MDA-MB-231[c], MG-63[d], U87MG[e], PC3[f], HeLa[g] and Vero[h] cells determined by the MTT assay.

Code	HT-29[b]	MDA-MB-231[c]	MG-63[d]	U87MG[e]	PC3[f]	HeLa[g]	Vero[h]
8aa	>10	>10	5.86±0.25	6.06±0.15	5.06±0.20	2.66±0.58	-
8ab	>10	>10	>10	3.86±0.20	>10	>10	-
8ac	>10	>10	>10	>10	4.73±0.20	>10	-
8ad	>10	>10	>10	>10	>10	>10	-
8ae	>10	>10	>10	4.43±0.20	>10	>10	-
8ba	>10	>10	>10	4.36±0.11	>10	>10	-
8bb	>10	>10	>10	>10	4.30±0.55	4.53±0.20	-
8bc	>10	>10	7.13±0.35	>10	4.83±0.35	>10	-
8bd	>10	>10	>10	>10	5.30±0.10	>10	-
8be	>10	>10	>10	>10	>10	5.53±0.30	-
8ca	>10	>10	>10	>10	>10	>10	-
8cb	>10	>10	>10	>10	>10	>10	-
8cc	>10	>10	>10	5.23±0.15	4.70±0.10	7.33±0.30	-
8cd	>10	>10	8.00±0.17	4.50±0.30	3.36±0.15	>10	-
8ce	>10	>10	>10	5.36±0.25	4.70±0.10	>10	-

8da	>10	>10	>10	>10	>10	>10	-
8db	>10	>10	>10	>10	>10	>10	-
8dc	>10	>10	7.5±0.30	>10	>10	>10	-
8dd	>10	>10	8.43±0.49	>10	5.10±0.10	>10	-
8de	>10	>10	7.96±0.40	>10	>10	>10	-
8ea	11.32±0.47	>10	3.93±0.15	>10	7.30±0.43	>10	-
8eb	13.20±0.52	>10	4.09±0.11	4.90±0.20	4.20±0.30	>10	-
8ec	8.20±0.52	>10	**2.80±0.10**	3.90±0.20	3.36±0.32	>10	9.95±0.66
8ed	10.10±0.36	>10	**0.59±0.28**	4.20±0.30	>10	>10	8.41±0.16
8ee	>10	>10	8.20±0.30	>10	4.47±0.33	>10	-
8fa	>10	>10	>10	>10	>10	>10	-
8fb	>10	>10	>10	>10	>10	>10	-
8fc	>10	>10	8.06±0.51	>10	>10	>10	-
8fd	4.70±0.65	>10	9.56±0.20	7.36±0.20	>10	>10	-
8fe	>10	>10	10.30±0.20	8.16±0.35	>10	>10	-
Doxorubicin	1.38±0.04	1.20±0.32	2.54±0.20	-	1.20±0.14	1.72±0.16	-
Harmine	4.26±1.18	12.26±0.64	36.33±0.42	-	22.44±1.64	16.18±1.02	-

[a] Each data represents mean ± S.D. from three different experiments performed in triplicate.
[b] HT-29: human colon cancer cell line. [c] MDA-MB-231: human breast cancer cell line. [d] MG-63: human bone osteosarcoma cell line. [e] U87 MG: human brain cancer cell line. [f] PC3: human prostate cancer cell line. [g]HeLa: Human cervical cancer cell line. [h]Vero: normal monkey kidney cell line.

2.2.2. Topoisomerase II inhibition assay

Topoisomerases are the enzymes that involve in increasing or decreasing the winding of DNA. They control the topology of the DNA and play a significant role in DNA replication, transcription and segregation as well as recombination phenomena [22]. Two types of topoisomerases, Topo I and Topo II are well known. Type I, topoisomerases (Topo I) make a single nick in DNA strand while type II, topoisomerases (Topo II) make similar nicks on both the strands of the DNA. Topo II is a nuclear enzyme that influences the DNA topology by catalyzing the DNA cleavage and by religating the phosphodiester bonds and as a result, the

Topo II initiates multiple recombination/repair pathways that may leads to cell death [23]. The catalytic cycle of Topo II takes place in six different steps like (1) binding of Topo II to DNA, (2) double-stranded cleavage of the DNA, (3) ATP-dependent DNA strand passage, (4) religation of the cleaved DNA, (5) ATP hydrolysis and (6) enzyme recycling [24]. Topo II inhibition studies were carried out by using Topo II Drug Screening Kit (TG 1009, Topogen, USA). Catenated DNA kinetoplast DNA (kDNA) and topo II enzyme (5 units) was incubated in presence 10 μM Etoposide for 30 min (lane 3 in **Fig. 3**), which is considered as a positive control in the present experiment. These experimental results revealed that decatenation did not take place (by forming minicircles) and the ternary complex (kDNA+topo II and Etoposide complex) remained close to the origin. Similar studies when repeated with catenated kDNA (200–300 ng) in the presence of 10 μM **8ed** and **8ec** (lane 4 and 5 respectively in **Fig. 3**) revealed that due to the formation of ternary complex (kDNA+topo II and **8ec** and **8ed**) most of the DNA in the presence of **8ec** and **8ed** derivatives, remained near the origin and did not enter into the agarose gel. Further it is noticed that, with **8ec**, formation of ternary complex (kDNA+topo II and **8ec**) is less compared to **8ed**, indicating lesser topo II inhibition by **8ec** compared to **8ed**.These results are supported by the spectroscopy experimental results as well as the K_d values calculated using the UV-vis abosorption data, which shows that **8ed** has better interaction with DNA compared to **8ec**. The results indicate that in the absence of derivatives, kDNA remained in the catenated form (lane 1) and on addition of topo II, the kDNA has transformed into decatenated form (lane 2) as depicted in **Fig. 3**. From these studies it is evident that the two derivatives considered in the present work (mainly **8ec** and **8ed**) inhibit topo II activity.

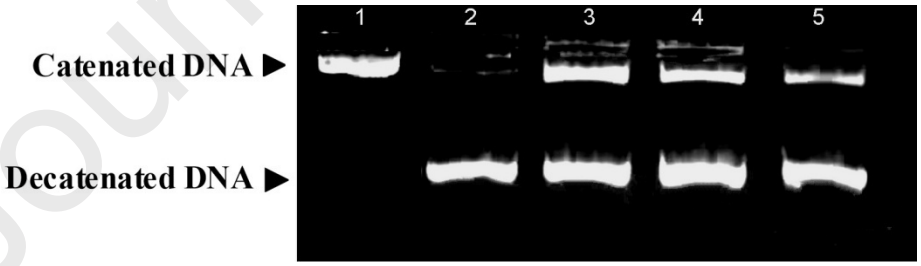

Fig. 3. Topo II inhibition assay. To about 200–300 ng of kDNA, about 5 units of Topo II was added and incubated at 37°C for 30 min. Lane 1- kDNA alone; Lane 2- kDNA and topo II; Lane 3- kDNA, topo II and Etoposide; Lane 4- kDNA, topo II and **8ed**; Lane 5- kDNA, topo II and **8ec**.

2.2.3. Apoptosis induction studies

2.2.3.1. Cell cycle analysis

In order to validate the results obtained from MTT assay as well as to understand the effect of **8ec** and **8ed** on cell cycle progression, cell cycle analysis was performed, wherein MG-63 cells were treated with **8ed** (0.5 µM) and **8ec** (2 µM) for 24 h and then the cells were stained with propidium iodide and further analyzed by using BD FACSVerseTM flow analyzer. There was a significant increase in the population of cells at sub G1 phase was observed with respect to control cells. The results obtained from **Fig. 4** clearly indicated that MG-63 untreated control cells showed 1.05% cells in sub G1 phase, whereas compound **8ed** showed 6.95% and **8ec** showed 8.02% of cell accumulation in sub G1 phase. These results imply that active congeners **8ed** and **8ec** arrest the cell cycle at sub G1 phase thereby induces apoptosis.

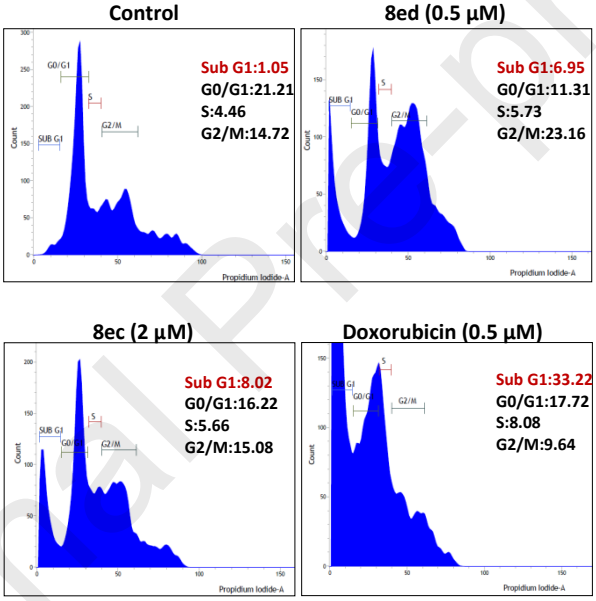

Fig. 4. Effect of **8ed** (0.5 µM) and **8ec** (2 µM) on cell cycle progression of MG-63 and assay was performed after 24 h. The analysis of cell cycle distribution was performed by using propidium iodide staining method.

2.2.3.2. Phase contrast microscopy

To examine whether the treatment with most active congeners **8ed** and **8ec** may lead to induction of apoptosis, MG-63 cells were treated with active compounds. After 48 h of incubation, images were captured in phase contrast microscopy which is depicted in **Fig.5 (i)** whereas characteristic morphological features such as shrinkage of cells, membrane blebbing, detachment from substratum, reduction in number of viable cells was observed in treated

cells compared to the untreated control cells. The same results were observed with doxorubicin.

2.2.3.3. Acridine orange/ethidium bromide (AO/EB) staining

The morphological changes induced by the active compounds **8ed** and **8ec** in MG-63 cells were further studied by using acridine orange/ethidium bromide (AO/EB) staining technique. AO penetrate through the intact cell membrane and stains the nuclei in green, whereas EB can stains the nuclei of cells in red that have lost membrane integrity and necrotic cells. It can be inferred from **Fig. 5 (ii)** that control cells appeared in green colour due to its normal morphology. Treated MG-63 cells (**8ed** and **8ec)** demonstrate the morphological changes such as membrane blebbing, cell shrinkage, chromatin condensation and apoptotic body formation indicating that the compounds induce apoptosis.

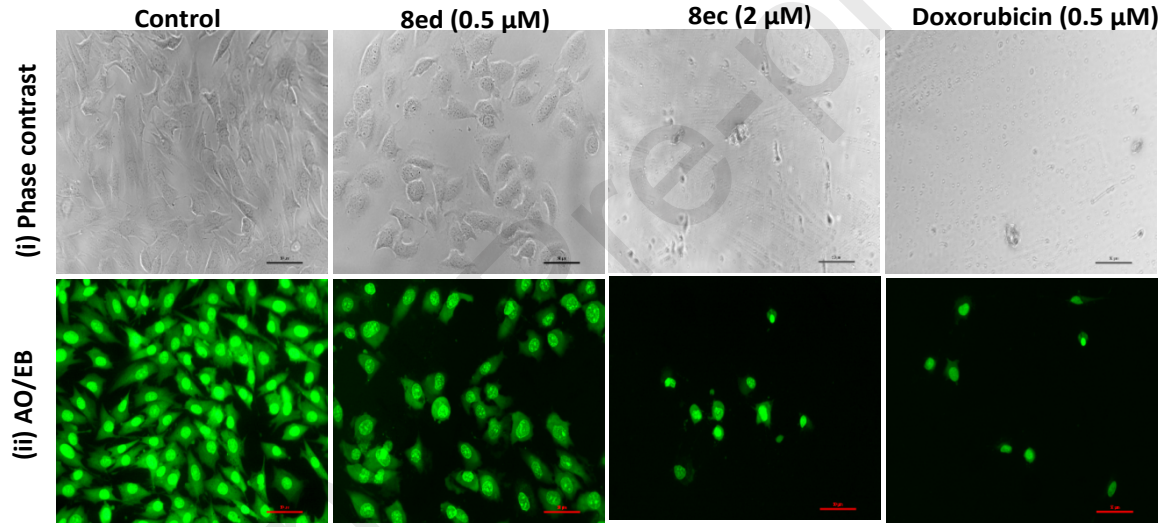

Fig. 5. (i) Morphological changes observed in MG-63 cells were treated with and without compound **8ed** (0.5 µM) and **8ec** (2µM). After 48 h the images were captured with a phase contrast microscope (200x magnification, scale bar = 50 µm). (ii) AO/EB staining in MG-63 cells treated with and without compound **8ed** (0.5 µM) and **8ec** (2µM) for 48 h and compared with control and standard drug (Doxorubicin).

2.2.3.4. DAPI staining

The characteristic feature of apoptotic cells is condensation of nucleus and it can be observed by DAPI nuclear staining method [25]. DAPI (4',6-diamidino-2-phenylindole) is a blue fluorescent dye, which can pervade intact membrane of live cells and stains the nucleus in light blue, wherein the apoptotic cell nuclei appears as bright blue due to chromatin condensation. MG-63 cells were stained with DAPI followed by the treatment with both the compounds **8ed** (0.5 µM) and **8ec** (2 µM), there by cells were observed under fluorescence

microscope for nuclear morphological changes. The results observed from **Fig.6 (i)** that control cells were intact with normal morphology, while treated compounds **8ed** and **8ec** led to the nuclear changes like horse-shoe shaped, chromatin condensation, pyknotic or fragmented bright nuclei. From the results, it was evident that these compounds **8ed** and **8ec** had induced apoptosis in MG-63 cells.

2.2.3.5. Measurement of reactive oxygen species (ROS)

In order to determine the ability of compound **8ed** (0.5 µM) and **8ec** (2 µM) on the ROS generation, the intracellular ROS levels were examined by using DCFDA staining assay [26]. DCFDA (2',7'-dichlorofluorescin diacetate) is a non-fluorescent probe which is readily oxidized to 2',7'-dichlorofluorescein (DCF) in the presence of ROS. MG-63 cells were treated with compound **8ed** and **8ec** at indicated concentrations, significant increase in the green fluorescence was observed which is comparable with Doxorubicin. These results clearly state that induction of ROS by the treated compounds is one of the prompting mechanism to induce apoptosis in MG-63 cells (**Fig.6 (ii)**).

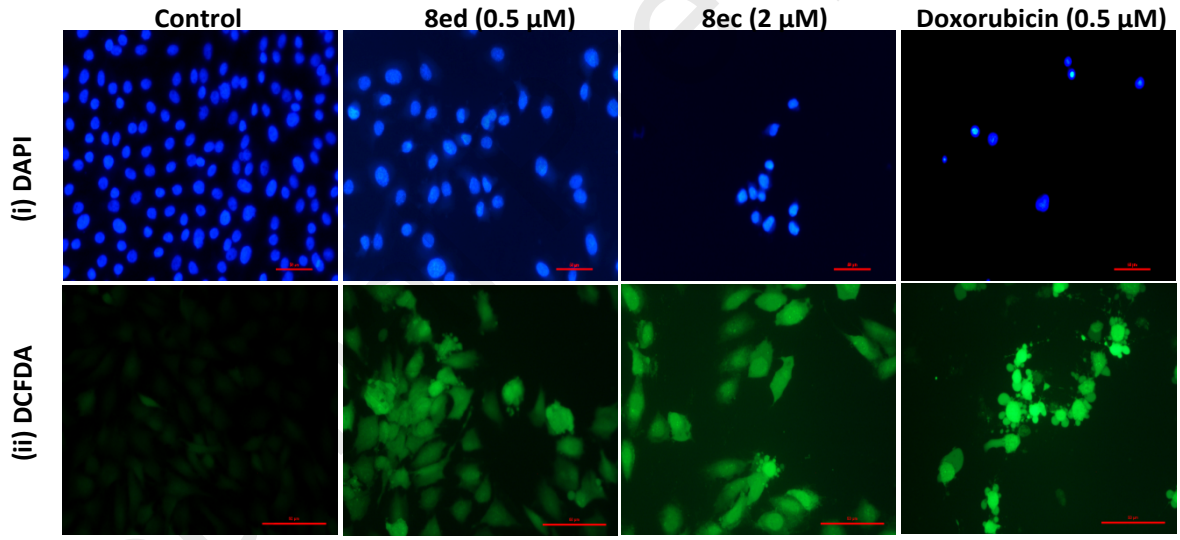

Fig. 6. (i) Nuclear morphology of cancer cells after DAPI staining. MG-63 cells treated with and without compound **8ed** (0.5 µM) and **8ec** (2 µM) for 48 h and compared with control and Doxorubicin. The images were captured with fluorescence microscope (200x magnification, scale bar = 50 µm). (ii) DCFDA staining in MG-63 cells treated with and without compound **8ed** (0.5 µM) and **8ec** (2 µM) for 24 h and compared with control and standard drug (Doxorubicin).

2.2.3.6. Effect on mitochondrial membrane potential (ΔΨm)

Mitochondria play a key role in initiating the intrinsic apoptotic pathway. To further evaluate the effect of compound on mitochondria, ΔΨm was measured. JC-1 is a lipophilic cationic dye was used to evaluate ΔΨm, in which polarized mitochondria stains red due to formation of J-aggregates, while depolarised mitochondria in apoptotic cells stains green because of J-monomers. MG-63 cells were treated with **8ed** (0.5 µM) and **8ec** (2 µM) for 48 h and remarkable increase in the mitochondrial membrane depolarisation was observed as compared to control cells as shown in the **Fig.7**. Flow-cytometric analysis of the treated cells clearly displayed an increase in depolarized cell population (P2) from 1.42% in control to 14.15%, 19.20% for **8ed** (0.5 µM) and **8ec** (2 µM) respectively. Thus, the treated compounds clearly induced the loss of mitochondrial membrane potential and suggest the involvement of mitochondria dependent apoptotic pathway in the mechanism of action.

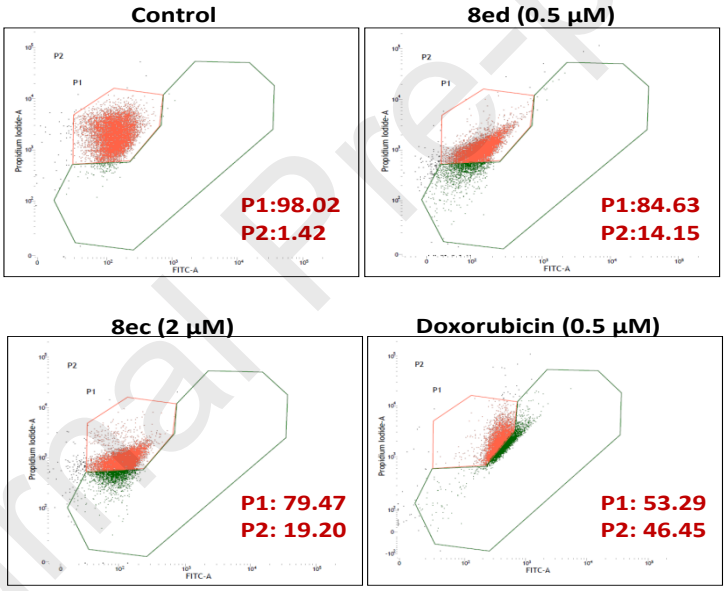

Fig. 7. Effect on mitochondrial membrane potential. MG-63 cells were treated with **8ed** and **8ec** for 48 h and JC-1 staining was performed. The control represents the cells without compound.

2.2.3.7. Annexin V-Alexa fluor 488/PI assay

To quantify the percentage of apoptotic cell death induced by the compound **8ed** (0.5 µM) and **8ec** (2 µM) on MG-63 cells, Alexa Fluor 488 annexin V/Propidium iodide staining assay was performed. MG-63 cells were treated with compound **8ed** (0.5 µM) and **8ec** (2 µM) for 48 h and stained with Annexin V-alexa fluor488 and propidium iodide, and samples were analysed by flow cytometry. Annexin assay ease the detection of necrotic cells (Q1-UL; AV-

/PI+), live cells (Q2-LL; AV-/PI-), early apoptoticcells (Q3-LR; AV+/PI-), and late apoptotic cells (Q4- UR;AV+/PI+). Results from **Fig. 8** indicate compound **8ed** and **8ec** induce apoptosis in comparison to control.

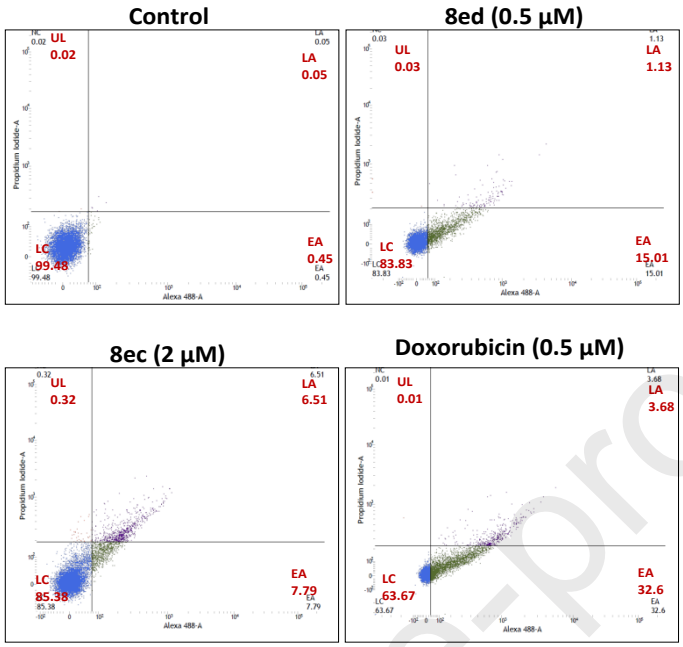

Fig. 8. Effect of compound on cell apoptosis as measured by Annexin V-Alexa fluor /propidium iodide staining assay. MG-63 cells were treated with compound **8ed** (0.5 µM) and **8ec** (2 µM) for 48 h. Then 10,000 cells from each sample were analyzed by flow cytometry. The percentage of cells positive for Annexin V-Alexa fluor 488 and/or Propidium iodide is represented inside the quadrants.

2.2.4. DNA binding studies

To further ratify the biological activities of these potential congeners (**8ec** and **8ed)** and to understand the mode of interaction with DNA, spectroscopic studies such as UV-visible, fluorescence, circular dichroism spectroscopy and viscosity studies were performed.

2.2.4.1. UV-visible Spectroscopic Studies.

In order to find the interaction of **8ec** and **8ed** with double stranded DNA, UV-visibility spectroscopy study was carried out. However, both these derivatives have shown maximum absorption bands at around 208 nm and 206 nm with **8ec** and **8ed** respectively. But, upon addition of equal ratio of CT-DNA solution to the compounds, the absorption peak exhibited gradual hyperchromicity. Further, it is understood that very less hyperchromicity and no shift in the absorption peak is observed on interaction of CT DNA with each of these derivatives.

Each time after the successive addition of CT-DNA to **8ec** and **8ed** solution, samples were equilibrated for 5 min prior to measurement. The data obtained is fitted to Eq.(1), to obtain the dissociation constant (K_d) taking into account the total amount of 1:1 complex formed,independently of the derivative binding site(s).

K_d = [CT- DNA] [**8ec**/**8ed** compound] / [CT-DNA. **8ec**/**8ed** compound] ---------- (1)

From the absorbance values obtained when **8ec** and **8ed** compounds interact with CT-DNA, *dissociation constant* (K_d) was calculated using eq 1. The K_d values obtained on interaction of **8ec** and **8ed** with CT- DNA are 37 μM and 42 μM, respectively. Even K_d values obtained will indicate that **8ed** has marginally better binding with CT-DNA compared to **8ec**. From the experimental data, it is understood that **8ec**and **8ed** compounds are interacting moderately with CT DNA. But, it is difficult to conclude the nature and mode of binding of compounds with CT DNA only by UV-visible titration. The UV-visible spectra obtained on interaction of these derivatives with CT-DNA were shown in **Fig.9**.

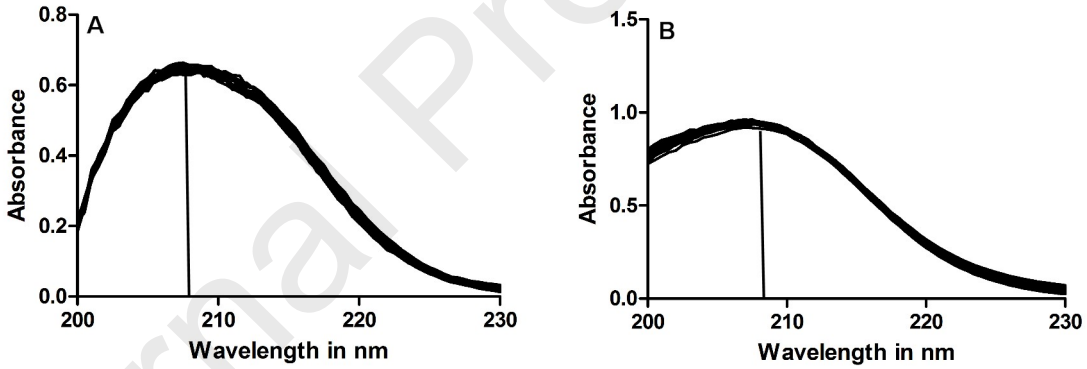

Fig. 9. UV-visible spectra obtained when **8ec**and **8ed** compounds interact with CT DNA**.** 25 μM of **8ec**and **8ed** compounds was taken in 1 cm path length cuvette and equal increments of CT DNA were added to cuvette. (A) The UV-vis spectra recorded with increasing concentration of CT DNA added to 25 μM of **8ec**. (B) The UV-vis spectra recorded with increasing concentration of CT DNA added to 25 μM of **8ed**.

2.2.4.2. Fluorescence spectroscopy

Fluorescence spectroscopy is another valuable biophysical technique to understand the binding mode of small molecules with DNA and to study the electronic environment around the DNA-complex at comparably lower concentrations [27]. The nature of interaction of compounds with DNA can be monitored at low concentration when they are fluorescent.

However, the emission spectra of compounds **8ec** and **8ed** shows a prominent peak in the range from 700-770 nm for **8ec** and from 370-670 nm for **8ed**. The compounds **8ec** and **8ed** are excited at 375 nm and 275 nm respectively. It is noticed that the derivatives fluorescence emission intensity has reduced gradually upon equal addition of CT DNA. The reduction in fluorescence intensity of **8ec** and **8ed** compounds with the addition of CT DNA, may be either due to the absorption of fluorescence emission energy by the DNA bases which are in the closely located to conjugate molecules or due to the absorption of emission energy by the surrounding water molecules. The degree of fluorescence quenching is comparatively high in case of **8ed** than **8ec**. The fluorescence spectrum of **8ec** and **8ed** with CT-DNA was shown in **Fig. 10**.

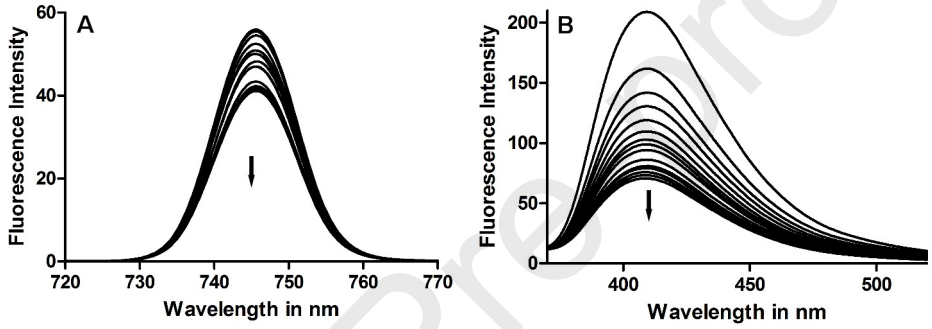

Fig. 10. Fluorescence spectra recorded when **8ec** and **8ed** compounds interact with CT DNA**.** 10 μM of **8ec** and **8ed** compounds was taken in 1 cm path length cuvette and equal increments of CT DNA (multiples of 0.5 μM) were added to cuvette. The compounds **8ec** and **8ed** were excited at 375 nm and 275 nm respectively and emission spectrum was recorded. (A) The fluorescence spectra recorded with increasing concentration of CT DNA added to 25 μM of **8ec**. (B) The fluorescence spectra recorded with increasing concentration of CT DNA added to 25 μM of **8ed**.

2.2.4.3. Circular Dichroism Studies

Further, to understand the effect of both **8ec** and **8ed** compounds on the conformation of CT DNA, circular dichroism (CD) studies are performed. The CD spectra of CT-DNA alone exhibited positive and negative bands around 270 nm and 240 nm respectively. On addition of 10 μM of **8ec** and **8ed** compounds to CT-DNA (conjugate/DNA, 1:1 ratio), the positive CD band exhibited hypochromicity, indicating unwinding of CT-DNA on interaction with *β*-carboline linked aryl sulfonyl piperazine congeners. Further, on increasing the concentration of **8ec** and **8ed** (conjugate /DNA, 2:1 ratio), the positive CD band intensity reduced further and exhibited slight red shift. These changes can be attributed to absorption flattening and

differential scattering phenomena. The representative CD spectra obtained with **8ec** and **8ed** compounds and CT-DNA were shown in **Fig. 11.**CD studies indicate that *β*-carboline linked aryl sulfonyl piperazine compounds interact with DNA and this can exhibit changes in DNA conformation. The positive CD band hypochromicity is more with **8ed** compared to **8ec**.Also, the negative CD band intensities reduced with both the compounds**8ec** and **8ed** indicating alteration in the DNA helicity. However maximum change was noticed with **8ed**. From the CD data it is evident that *β*-carboline linked aryl sulfonyl piperazine congeners alter the DNA helix on its interaction with CT-DNA, which is clear from the changed negative CD band intensities.

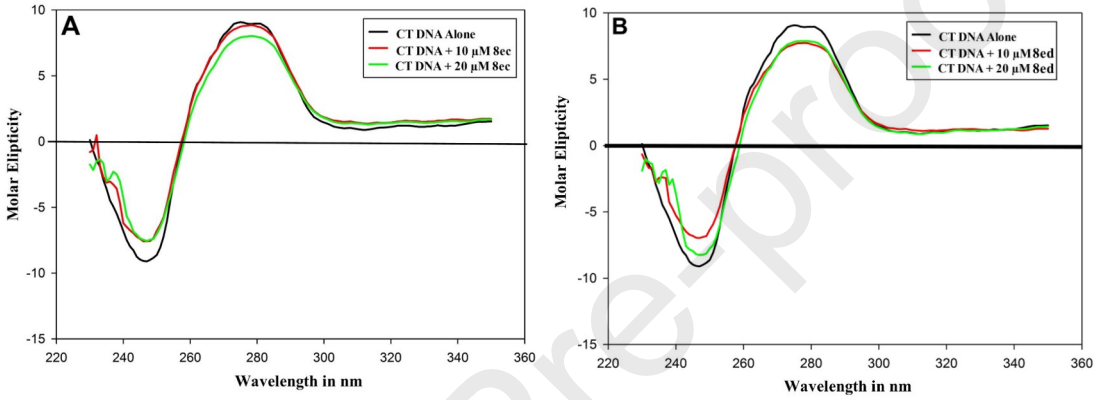

Fig. 11. Circular Dichroism profiles of CT DNA in 100 mM Tris-HCl (pH 7.0) in the absence or presence of **8ec** and **8ed** compounds. The conformational changes in CT DNA was observed when 10.0 µM and 20 µM of **8ec** and **8ed** compounds interact with 10.0 µM CT DNA (1:1 and 1:2 ratio of DNA:conjugate) in 1 cm path length cuvette. The spectra were averaged over 3 scans. (**A)** The CD spectra recorded when 10.0 µM and 20 µM **8ec** interact with 10.0 µM CT DNA. (B) The CD spectra recorded when 10.0 µM and 20 µM **8ed** interact with 10.0 µM CT DNA.

2.2.4.4. Viscosity studies

From the spectroscopic studies, it was clear that, the active compounds **8ec** and **8ed** interact well with CT DNA. Further, to conclude the nature and mode of interaction of **8ec** and **8ed** with CT DNA, viscosity studies were also carried out. The relative viscosity of DNA generally increases when the molecule intercalate with DNA. The enhanced viscosity may be due to the increase in the axial length of DNA helix on molecule's intercalation. Hence, intercalation of a molecule results in an increase in the viscosity of DNA solution [28]. Whereas, reduction in the relative viscosity is typically observed with covalent DNA binding [29] molecules. Moreover, viscosity does not change or show slight change when molecules bind to the surface of DNA [30].

In the case of active compounds **8ec** and **8ed**, the viscosity of DNA solution increased slowly with the addition of derivatives. But the variation in DNA viscosity on interaction of these compounds with DNA, is in between ethidium bromide (EtBr) and Hoechst 33342. Among both the derivatives, slight change in viscosity was observed in case of **8ed** compared to **8ec,** while with the ethidium bromide (EtBr), the viscosity of DNA has increased continuously as EtBr is a well known intercalator. The variation was less with the addition of Hoechst 33342, due to its binding to the groove. The viscosity change noticed on interaction of different molecules with CT is shown in **Fig. 12**. All the spectroscopic results and viscosity study results indicate that the **8ec** and **8ed** compounds interact well with DNA and they may bind to the surface of CT DNA.

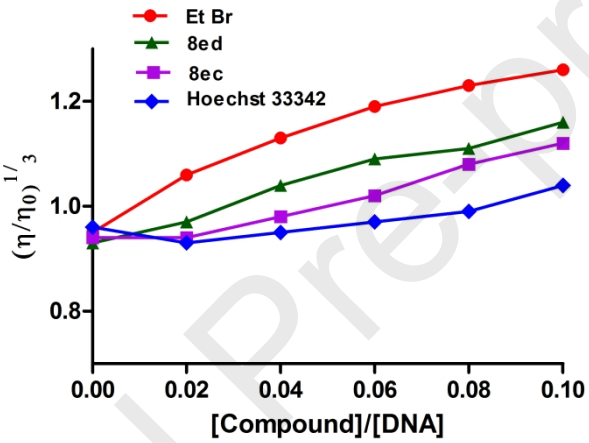

Fig. 12. Viscosity studies graphical representation of **8ec** (15 µM) and **8ed** (15 µM) compounds with CT-DNA solution (150 µM) at 25 °C, EtBr and Hoechst 33342 were used as controls.

2.3. Molecular Docking Studies

Molecular docking simulations were performed on biologically most active compounds of synthesized analogues i.e, *β*-carboline linked aryl sulfonyl piperazine derivatives (compound **8ed** and **8ec**) against the ATP binding domain of human topoisomerase IIα (PDB ID: 1ZXM) [31] using GLIDE docking module of Schrödinger suite 2017-1[32].

The binding mode of compounds**8ed** and **8ec** atthe ATP binding domain of human topoisomerase IIα was depicted in **Fig. 13.** Compound **8ed** has shown two hydrogen bond interactions with ATP binding domain residues of human topoisomerase IIα. The *β*-carboline NH- group of conjugate**8ed** has made strong hydrogen bond interaction with side chain of Asp99 with a distance of 2.79 Å. Carbonyl group of conjugate **8ed** has formed hydrogen bond interaction with side chain of Arg98 with a distance of 2.99 Å. As well, sulfonyl phenyl

moiety has made π-cation interaction with Arg98 and Lys157. In addition, a number of hydrophobic interactions were observed between conjugate**8ed** and ATP binding domain residues i.e Ile33, Tyr34, Pro100, Pro126 and Tyr186 which will enhances the binding of conjugate **8ed** in the ATP binding pocket of human topoisomerase IIα. In case of conjugate **8ec**, it has shown strong hydrogen bond interaction with Arg98. The *β*-carboline NH- and carbonyl group has established hydrogen bond interaction with back bone and side chain of Arg98, respectively in a two point contact way with a distance 2.19 Å and 2.97 Å. The *β*-carboline moiety also formed π-cation contact with Arg98. Furthermore, numerous hydrophobic contacts were also noticed between conjugate **8ec** and ATP binding domain residues which promotes the binding of **8ec** in theATP binding domain of hTopoIIα.

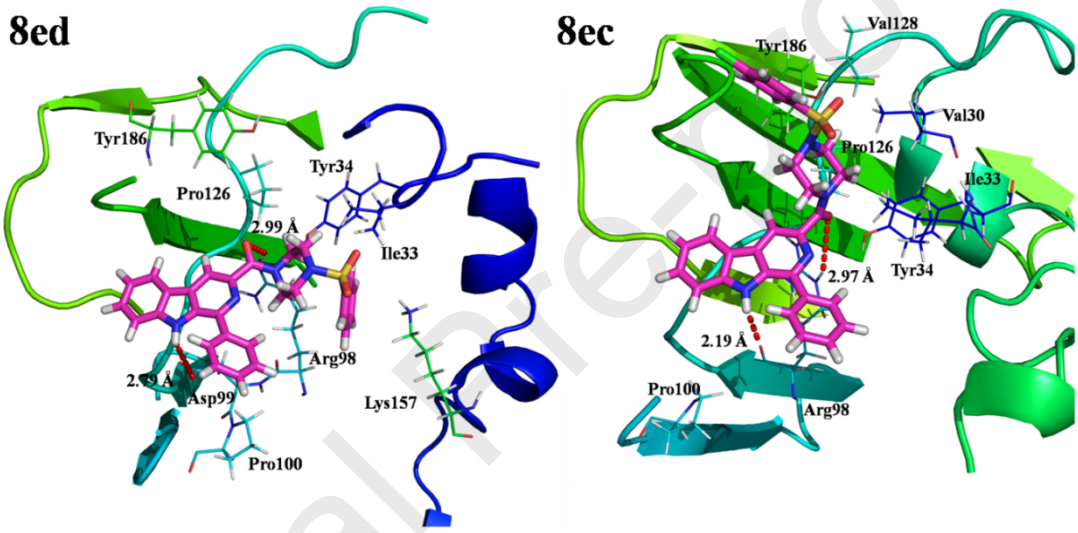

Fig. 13. View of compounds**8ed** and **8ec** docked in the ATP binding pocket of human topoisomerase IIα. The red dashed line represents hydrogen bond.

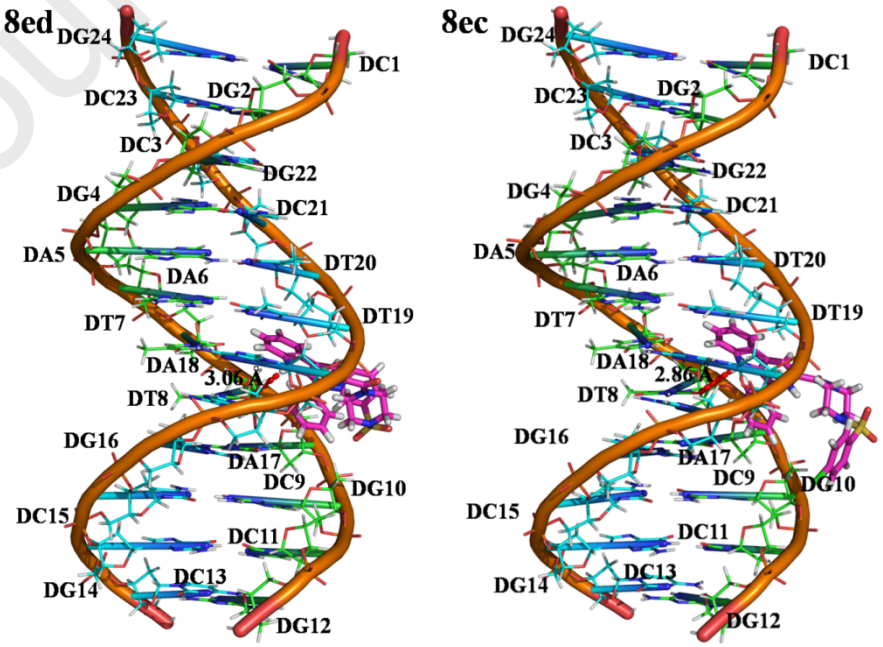

Fig. 14. Binding poses of compounds **8ed** and **8ec** in the minor groove of d(CGCGAATTCGCG)$_2$.

Additionally, molecular docking simulation studies were also performed to enumerate the binding mode of compounds **8ed** and **8ec** into the DNA duplex d(CGCGAATTCGCG)$_2$ (PDB ID: 1DNH) [33]. **Figure 14** illustrate the docking pose of compounds **8ed** and **8ec** at the minor groove of duplex DNA. The *β*-carboline NH- group of compounds **8ed** and **8ec** has established strong hydrogen bond interaction with **DT8** base pair of DNA with the distance of 3.06 Å and 2.86 Å, respectively. Further, the aromatic ring of the *β*-carboline moiety of compounds**8ed** and **8ec** were observed to be involved in π-π stacking interaction with the base pairs of DNA. All these interactions certainly stabilizes the binding of compounds**8ed** and **8ec** in the minor groove binding site of DNA duplex d(CGCGAATTCGCG)$_2$.

3. Conclusion

In conclusion, we have designed and synthesized a new series of *β*-carboline linked aryl sulfonyl piperazine compounds, possessing a substituted phenyl at position-1 and aryl sulfonyl piperazine motif at position-3 of the *β*-carboline moiety. These active compounds involving two pharmacophoric features and their cytotoxic property were evaluated against various human cancer cell lines. Compounds**8ec** and **8ed** showed profound cytotoxic activity against MG-63 cell line and induced apoptosis. Cell cycle analysis revealed that compounds**8ec** and **8ed** arrest at sub G1 phase. In addition these compounds inhibit efficiently topo II enzymatic activity by catalytic inhibition of topo II. The DNA binding studies states that **8ec** and **8ed** interact well with DNA and they may bind to the surface of CT DNA. Further docking studies are well correlated with the spectroscopic, viscosity studies and topo II inhibition studies. Therefore, all these studies are important to understand the role of pharmacophores and these hybrids have the potential to be developed as lead moleculesand suitable structural modifications may ensue in promising anticancer activity.

4. Experimental section

4.1. Materials and methods

All Chemicals and reagents were purchased from the commercial suppliers Alfa Aesar, Sigma Aldrich and used without further purification. The reaction progress was monitored by Thin layer chromatography (TLC) was performed using pre-coated silica gel 60 F_{254} MERCK. TLC plates were visualized and analysed by exposure to UV light or iodine vapors

and aqueous solution of ninhydrin. Column chromatography was performed with Merck flash silica gel with 60–120 mesh size. Melting points were determined on an Electro thermal melting point apparatus and are uncorrected. Nuclear magnetic resonance spectra for ^{1}H NMR were obtained on Avance 300, 400 and 500 MHz and analyzed using Mestrenova software and the chemical shifts are reported in ppm from tetramethylsilane (0 ppm) or the solvent resonance as the internal standard ($CDCl_3$ 7.26 ppm, DMSO-d_6 2.49 ppm) and for ^{13}C NMR the chemical shifts are reported in ppm from the solvent resonance as the internal standard ($CDCl_3$ 77 ppm, DMSO-d_6 39.3 ppm). Spin multiplicities are described as s (singlet), br s (broad singlet), d (doublet), dd (double doublet), t (triplet), td (triple doublet), q (quartet), or m (multiplet). Coupling constants are reported in hertz (Hz). Mass spectra were recorded by electrospray ionization mass spectrometry (ESI-MS). HRMS was performed on a Varian ESI- QTOF instrument.

4.2. General synthetic procedure for the preparation of compounds 8aa–fe

To a solution of amine intermediates (**7a–e**, 1 mmol) and appropriate *β*-carboline acid (1 mmol) in DMF(5 mL) was added EDCI (1.2 mmol), HOBt (1.2 mmol) and DIPEA (3 mmol) under nitrogen atmosphere and the reaction mixture was stirred at room temperature for 12 h. After the complete consumption of starting materials (monitored by TLC), reaction mixture was poured into ice-cold water (25 mL), extracted by EtOAc (3 × 30 mL) and the combined organic phases were washed with brine (20 mL), dried over anhydrous Na_2SO_4, filtered and concentrated in vacuo. The obtained residue was purified by column chromatography using EtOAc/*n*-hexane, collected fractions were evaporated in vacuo to afford the titled products **8aa–fe**.

4.2.1. (4-((4-Methoxyphenyl)sulfonyl)piperazin-1-yl)(1-(4-(trifluoromethyl)phenyl)-9*H*-pyrido[3,4-*b*]indol-3-yl)methanone (8aa)

White solid:88% yield; mp: 254–256 °C;^{1}H NMR (300 MHz, DMSO-d_6) δ: 11.91 (s, 1H), 8.50 (s, 1H), 8.34 (d, J = 7.8 Hz, 1H), 8.19 (d, J = 7.9 Hz, 2H), 7.99 (d, J = 8.0 Hz, 2H), 7.71 (d, J = 8.7 Hz, 2H), 7.63 (dd, J = 16.3, 7.7 Hz, 2H), 7.29 (t, J = 7.4 Hz, 1H), 7.14 (d, J = 8.7 Hz, 2H), 3.83 (s, 7H), 2.98 (s, 4H); ^{13}C NMR (75 MHz, DMSO-d_6) δ: 167.4, 162.8, 142.1, 141.7, 141.5, 138.4, 133.5, 130.1, 129.8, 129.3, 128.8, 126.0, 125.6, 122.5, 122.0, 120.8, 120.1, 115.8, 114.5, 112.5, 111.3, 55.6, 46.3, 41.3; MS (ESI): *m/z* 595 $[M+H]^+$; HRMS (ESI): *m/z* calcd for $C_{30}H_{26}F_3N_4O_4S$: 595.16214; found: 595.16442 $[M+H]^+$.

4.2.2. (4-Tosylpiperazin-1-yl)(1-(4-(trifluoromethyl)phenyl)-9*H*-pyrido[3,4-*b*]indol-3-yl)methanone (8ab)

Cream solid:85% yield; mp: 275–277 °C; ^{1}H NMR (300 MHz, DMSO-d_6) δ: 11.84 (s, 1H), 8.45 (s, 1H), 8.31–8.23 (m, 1H), 8.15 (d, J = 8.1 Hz, 2H), 7.94 (d, J = 8.2 Hz, 2H), 7.64 (d, J = 8.2 Hz, 3H), 7.56 (t, J = 7.6 Hz, 1H), 7.41 (d, J = 8.1 Hz, 2H), 7.28 (t, J = 7.4 Hz, 1H), 3.83 (s, 4H), 3.01 (s, 4H), 2.39 (s, 3H); ^{13}C NMR (101 MHz, $CDCl_3$+DMSO-d_6) δ: 167.3, 143.6, 142.0, 141.5, 141.4, 138.3, 133.3, 131.7, 130.1, 129.7, 129.2, 128.9, 128.7, 127.5, 125.4, 122.8, 121.8, 120.8, 120.1, 115.7, 112.4, 46.3, 41.3, 20.9; MS (ESI): *m/z* 579 $[M+H]^+$; HRMS (ESI): *m/z* calcd for $C_{30}H_{26}F_3N_4O_3S$: 579.16722; found: 579.16900 $[M+H]^+$.

4.2.3. (4-((4-Chlorophenyl)sulfonyl)piperazin-1-yl)(1-(4-(trifluoromethyl)phenyl)-9*H*-pyrido[3,4-*b*]indol-3-yl)methanone (8ac)

White solid:90% yield;mp: 258–260 °C; ^{1}H NMR (300 MHz, DMSO-d_6) δ: 11.91 (s, 1H), 8.51 (s, 1H), 8.35 (d, J = 8.0 Hz, 1H), 8.16 (d, J = 7.8 Hz, 2H), 8.00 (d, J = 8.0 Hz, 2H), 7.79 (d, J = 8.5 Hz, 2H), 7.71 (d, J = 7.1 Hz, 3H), 7.63 (d, J = 6.2 Hz, 1H), 7.31 (t, J = 7.0 Hz, 1H), 3.82 (s, 4H), 3.01 (s, 4H); ^{13}C NMR (101 MHz, DMSO-d_6) δ: 167.5, 142.2, 141.6, 141.5, 138.5, 138.4, 133.6, 133.4, 130.2, 129.6, 129.6, 129.4, 129.2, 128.9, 125.7, 123.0, 122.1, 120.9, 120.3, 115.9, 112.6, 46.4, 41.4; MS (ESI): *m/z* 599 $[M+H]^+$; HRMS (ESI): *m/z* calcd for $C_{29}H_{23}ClF_3N_4O_3S$: 599.11260; found: 599.11474 $[M+H]^+$.

4.2.4. (4-(Phenylsulfonyl)piperazin-1-yl)(1-(4-(trifluoromethyl)phenyl)-9*H*-pyrido[3,4-*b*]indol-3-yl)methanone (8ad)

White solid:84% yield; mp: 195–197 °C; ^{1}H NMR (300 MHz, DMSO-d_6) δ: 11.89 (s, 1H), 8.50 (s, 1H), 8.35 (d, J = 7.8 Hz, 1H), 8.16 (d, J = 7.9 Hz, 2H), 7.99 (d, J = 8.1 Hz, 2H), 7.77 (d, J = 7.5 Hz, 2H), 7.69–7.56 (m, 5H), 7.30 (t, J = 7.3 Hz, 1H), 3.82 (s, 4H), 3.02 (s, 4H); ^{13}C NMR (75 MHz, DMSO-d_6) δ: 167.4, 156.3, 142.2, 141.5, 138.4, 134.7, 133.4, 130.1, 129.4, 129.3, 128.9, 127.6, 125.6, 122.0, 120.8, 120.2, 117.8, 115.9, 112.5, 46.4, 41.3; MS (ESI): *m/z* 565 $[M+H]^+$; HRMS (ESI): *m/z* calcd for $C_{29}H_{24}F_3N_4O_3S$: 565.15157; found: 565.15315 $[M+H]^+$.

4.2.5. (4-((4-(Tert-butyl)phenyl)sulfonyl)piperazin-1-yl)(1-(4-(trifluoromethyl)phenyl)-9*H*-pyrido[3,4-*b*]indol-3-yl)methanone (8ae)

Cream solid:82% yield; mp: 191–193 °C;^{1}H NMR (300 MHz, DMSO-d_6) δ: 11.90 (s, 1H), 8.51 (s, 1H), 8.35 (d, J = 7.7 Hz, 1H), 8.15 (d, J = 7.9 Hz, 2H), 8.00 (d, J = 8.0 Hz, 2H), 7.71 (d, J = 8.2 Hz, 2H), 7.68–7.54 (m, 4H), 7.30 (t, J = 7.0 Hz, 1H), 3.81 (s, 4H), 3.03 (s, 4H), 1.27 (s, 9H); ^{13}C NMR (75 MHz, DMSO-d_6) δ: 167.3, 156.3, 142.2, 141.5, 139.5, 138.4, 133.3, 131.8, 130.1, 129.3, 128.8, 127.5, 126.1, 125.6, 122.0, 120.8, 120.2, 115.8, 112.5, 46.4, 34.8, 30.6; MS (ESI): *m/z* 621 $[M+H]^+$; HRMS (ESI): *m/z* calcd for $C_{33}H_{32}F_3N_4O_3S$: 621.21417; found: 621.21719 $[M+H]^+$.

4.2.6. (1-(4-Fluorophenyl)-9*H*-pyrido[3,4-*b*]indol-3-yl)(4-((4-methoxyphenyl)sulfonyl)piperazin-1-yl)methanone (8ba)

Cream solid:90% yield; mp: 186–188°C;^{1}H NMR (300 MHz, DMSO-d_6) δ: 11.81 (s, 1H), 8.43 (s, 1H), 8.32 (d, J = 7.7 Hz, 1H), 8.00 (dd, J = 8.2, 5.7 Hz, 2H), 7.70 (d, J = 8.7 Hz, 2H), 7.65 (s, 1H), 7.58 (t, J = 7.5 Hz, 1H), 7.48 (t, J = 8.8 Hz, 2H), 7.29 (t, J = 7.3 Hz, 1H), 7.16 (d, J = 8.7 Hz, 2H), 3.84 (s, 3H), 3.80 (s, 4H), 2.97 (s, 4H); ^{13}C NMR (75 MHz, DMSO-d_6) δ: 167.5, 164.1, 162.8, 142.0, 141.4, 139.1, 134.0, 133.0, 130.7 (d, J = 8.4 Hz), 129.8, 128.7, 126.0, 121.9, 120.9, 120.1, 115.8, 115.5, 115.1, 114.6, 112.5, 55.7, 46.4, 41.3; MS (ESI): *m/z* 545 $[M+H]^+$; HRMS (ESI): *m/z* calcd for $C_{29}H_{26}FN_4O_4S$: 545.16533; found: 545.16669 $[M+H]^+$.

4.2.7. (1-(4-Fluorophenyl)-9*H*-pyrido[3,4-*b*]indol-3-yl)(4-tosylpiperazin-1-yl)methanone (8bb)

White solid:85% yield; mp: 244–246°C;^{1}H NMR (300 MHz, DMSO-d_6) δ: 11.80 (s, 1H), 8.43 (s, 1H), 8.32 (d, J = 7.9 Hz, 1H), 8.00 (dd, J = 8.7, 5.6 Hz, 2H), 7.65 (dd, J = 8.2, 3.3 Hz, 3H), 7.58 (t, J = 7.2 Hz, 1H), 7.47 (t, J = 8.5 Hz, 4H), 7.28 (t, J = 7.4 Hz, 1H), 3.80 (s, 4H), 2.98 (s, 4H), 2.39 (s, 3H); ^{13}C NMR (126 MHz, DMSO-d_6) δ: 167.5, 161.5, 143.9, 142.0, 141.5, 139.2, 134.0, 133.0, 131.7, 130.7 (d, J = 8.3 Hz), 129.9, 129.8, 128.7, 127.6, 121.9, 120.9, 120.1, 115.7 (d, J = 21.6 Hz), 115.1, 112.5, 46.4, 46.0, 21.0; MS (ESI): *m/z* 529 $[M+H]^+$; HRMS (ESI): *m/z* calcd for $C_{29}H_{26}FN_4O_3S$: 529.17042; found: 529.17126 $[M+H]^+$.

4.2.8. (4-((4-Chlorophenyl)sulfonyl)piperazin-1-yl)(1-(4-fluorophenyl)-9*H*-pyrido[3,4-*b*]indol-3-yl)methanone (8bc)

White solid:82% yield; mp: 253–255°C;^{1}H NMR (300 MHz, DMSO-d_6) δ: 11.81 (s, 1H), 8.43 (s, 1H), 8.32 (d, J = 7.9 Hz, 1H), 8.00 (dd, J = 8.7, 5.5 Hz, 2H), 7.77 (s, 1H), 7.73 (d, J = 8.8 Hz, 2H), 7.70–7.63 (m, 2H), 7.58 (t, J = 7.2 Hz, 1H), 7.47 (t, J = 8.9 Hz, 2H), 7.29 (t, J =

7.0 Hz, 1H), 3.81 (s, 4H), 3.01 (s, 4H); ^{13}C NMR (75 MHz, DMSO-d_6) δ: 167.5, 164.1, 142.0, 141.4, 139.1, 138.4, 134.0, 133.6, 133.0, 130.7 (d, J = 8.5 Hz), 129.8, 129.6, 129.5, 128.7, 121.9, 120.9, 120.1, 115.7 (d, J = 21.5 Hz), 115.1, 112.5, 46.3, 41.3; MS (ESI): *m/z* 549 $[M+H]^+$; HRMS (ESI): *m/z* calcd for $C_{28}H_{23}ClFN_4O_3S$: 549.11579; found: 549.11733 $[M+H]^+$.

4.2.9. (1-(4-Fluorophenyl)-9*H*-pyrido[3,4-*b*]indol-3-yl)(4-(phenylsulfonyl)piperazin-1-yl)methanone (8bd)

White solid: 80% yield; mp: 232–234°C;^{1}H NMR (300 MHz, DMSO-d_6) δ: 11.80 (s, 1H), 8.43 (s, 1H), 8.32 (d, J = 7.9 Hz, 1H), 8.00 (dd, J = 8.8, 5.5 Hz, 2H), 7.80–7.75 (m, 2H), 7.69 (s, 1H), 7.68–7.63 (m, 3H), 7.62 – 7.54 (m, 1H), 7.47 (t, J = 8.9 Hz, 2H), 7.28 (t, J = 7.4 Hz, 1H), 3.81 (s, 4H), 3.01 (s, 4H); ^{13}C NMR (75 MHz, DMSO-d_6) δ: 167.5, 164.1, 160.8, 142.0, 141.4, 139.1, 134.6, 134.0, 133.4, 133.0, 130.6 (d, J = 8.4 Hz), 129.6 (d, J = 24.4 Hz), 128.6, 127.5, 121.9, 120.9, 120.1, 115.7 (d, J = 21.5 Hz), 115.1, 112.5, 46.4, 41.3; MS (ESI): *m/z* 515 $[M+H]^+$; HRMS (ESI): *m/z* calcd for $C_{28}H_{24}FN_4O_3S$: 515.15477; found: 515.15566 $[M+H]^+$.

4.2.10. (4-((4-(Tert-butyl)phenyl)sulfonyl)piperazin-1-yl)(1-(4-fluorophenyl)-9*H*-pyrido[3,4-*b*]indol-3-yl)methanone (8be)

White solid:84% yield; mp: 260–262°C;^{1}H NMR (300 MHz, DMSO-d_6) δ: 11.81 (s, 1H), 8.44 (s, 1H), 8.32 (d, J = 7.9 Hz, 1H), 7.97 (dd, J = 8.7, 5.5 Hz, 2H), 7.69 (d, J = 1.6 Hz, 4H), 7.65 (d, J = 2.9 Hz, 1H), 7.58 (t, J = 7.2 Hz, 1H), 7.47 (t, J = 8.9 Hz, 2H), 7.28 (t, J = 7.4 Hz, 1H), 3.81 (s, 4H), 3.01 (s, 4H), 1.28 (s, 9H); ^{13}C NMR (75 MHz, DMSO-d_6) δ: 167.5, 164.1, 160.8, 156.3, 142.0, 141.4, 139.1, 134.0, 133.0, 131.7, 130.7 (d, J = 8.4 Hz), 129.8, 128.7, 127.6, 126.3, 121.4 (d, J = 76.6 Hz), 120.1, 115.6 (d, J = 21.5 Hz), 115.1, 112.5, 46.4, 41.4, 34.9, 30.7; MS (ESI): *m/z* 571 $[M+H]^+$; HRMS (ESI): *m/z* calcd for $C_{32}H_{32}FN_4O_3S$: 571.21737; found: 571.21842 $[M+H]^+$.

4.2.11. (1-(4-Methoxyphenyl)-9*H*-pyrido[3,4-*b*]indol-3-yl)(4-((4-methoxyphenyl)sulfonyl)piperazin-1-yl)methanone (8ca)

White solid:88% yield; mp: 228–230°C;^{1}H NMR (500 MHz, DMSO-d_6) δ: 11.71 (s, 1H), 8.35 (s, 1H), 8.29 (d, J = 7.9 Hz, 1H), 7.90 (d, J = 8.7 Hz, 2H), 7.70 (d, J = 8.9 Hz, 2H), 7.66 (d, J = 8.2 Hz, 1H), 7.56 (t, J = 7.7 Hz, 1H), 7.27 (t, J = 7.5 Hz, 1H), 7.20–7.13 (m, 4H), 3.90 (s, 3H), 3.83 (s, 3H), 3.79 (s, 4H), 2.97 (s, 4H); ^{13}C NMR (101 MHz, DMSO-d_6) δ: 167.7,

162.9, 159.9, 142.0, 141.4, 140.1, 132.9, 130.1, 129.9, 129.8, 129.5, 128.5, 126.0, 121.9, 121.0, 120.0, 114.6, 114.5, 114.3, 112.6, 55.7, 55.4, 46.5, 41.3; MS (ESI): *m/z* 557 $[M+H]^+$; HRMS (ESI): *m/z* calcd for $C_{30}H_{29}N_4O_5S$: 557.18532; found: 557.18670 $[M+H]^+$.

4.2.12. (1-(4-Methoxyphenyl)-9*H*-pyrido[3,4-*b*]indol-3-yl)(4-tosylpiperazin-1-yl)methanone (8cb)

White solid:84% yield; mp: 148–150°C;^{1}H NMR (300 MHz, DMSO-d_6) δ: 11.73 (s, 1H), 8.37 (s, 1H), 8.30 (d, J = 7.9 Hz, 1H), 7.91 (d, J = 8.7 Hz, 2H), 7.65 (d, J = 8.1 Hz, 3H), 7.57 (t, J = 7.6 Hz, 1H), 7.46 (d, J = 8.0 Hz, 2H), 7.27 (t, J = 7.4 Hz, 1H), 7.19 (d, J = 8.7 Hz, 2H), 3.91 (s, 3H), 3.81 (s, 4H), 2.99 (s, 4H), 2.40 (s, 3H); ^{13}C NMR (75 MHz, DMSO-d_6) δ: 167.6, 159.8, 143.8, 141.9, 141.4, 140.0, 132.8, 131.7, 130.0, 129.9, 129.8, 129.5, 128.4, 127.6, 121.8, 121.0, 119.9, 114.5, 114.2, 112.6, 55.4, 46.4, 21.0; MS (ESI): *m/z* 541 $[M+H]^+$; HRMS (ESI): *m/z* calcd for $C_{30}H_{29}N_4O_4S$: 541.19040; found: 541.19162 $[M+H]^+$.

4.2.13. (4-((4-Chlorophenyl)sulfonyl)piperazin-1-yl)(1-(4-methoxyphenyl)-9*H*-pyrido[3,4-*b*]indol-3-yl)methanone (8cc)

White solid:88% yield; mp: 214–216°C;^{1}H NMR (300 MHz, DMSO-d_6) δ: 11.73 (s, 1H), 8.38 (s, 1H), 8.30 (d, J = 7.8 Hz, 1H), 7.92 (d, J = 8.5 Hz, 2H), 7.82–7.73 (m, 3H), 7.71–7.63 (m, 2H), 7.57 (t, J = 7.5 Hz, 1H), 7.27 (t, J = 7.4 Hz, 1H), 7.19 (d, J = 8.6 Hz, 2H), 3.91 (s, 3H), 3.82 (s, 4H), 3.01 (s, 4H); ^{13}C NMR (101 MHz, DMSO-d_6) δ: 167.6, 159.8, 141.9, 141.4, 140.0, 138.4, 133.6, 133.1, 132.8, 130.0, 129.8, 129.6, 129.5, 128.4, 121.8, 121.0, 119.9, 114.5, 114.2, 112.5, 55.4, 46.3, 41.3; MS (ESI): *m/z* 561 $[M+H]^+$; HRMS (ESI): *m/z* calcd for $C_{29}H_{26}ClN_4O_4S$: 561.13578; found: 561.13720 $[M+H]^+$.

4.2.14. (1-(4-Methoxyphenyl)-9*H*-pyrido[3,4-*b*]indol-3-yl)(4-(phenylsulfonyl)piperazin-1-yl)methanone (8cd)

White solid:82% yield; mp: 225–227°C; ^{1}H NMR (300 MHz, DMSO-d_6) δ: 11.72 (s, 1H), 8.37 (s, 1H), 8.30 (d, J = 7.9 Hz, 1H), 7.91 (d, J = 8.7 Hz, 2H), 7.76 (t, J = 8.5 Hz, 3H), 7.71–7.64 (m, 3H), 7.58 (dd, J = 14.5, 7.4 Hz, 1H), 7.27 (t, J = 7.3 Hz, 1H), 7.19 (d, J = 8.7 Hz, 2H), 3.91 (s, 3H), 3.81 (s, 4H), 3.02 (s, 4H); ^{13}C NMR (75 MHz, DMSO-d_6) δ: 167.6, 164.9, 159.8, 141.3, 140.1, 140.0, 133.4, 132.8, 130.0, 129.7, 129.4, 128.4, 127.5, 121.8, 120.9, 119.9, 114.5, 114.2, 112.5, 109.6, 55.3, 46.3; MS (ESI): *m/z* 527 $[M+H]^+$; HRMS (ESI): *m/z* calcd for $C_{29}H_{27}N_4O_4S$: 527.17475; found: 527.17565 $[M+H]^+$.

4.2.15. (4-((4-(Tert-butyl)phenyl)sulfonyl)piperazin-1-yl)(1-(4-methoxyphenyl)-9*H*-pyrido[3,4-*b*]indol-3-yl)methanone (8ce)

White solid:90% yield; mp: 145–147°C; ^{1}H NMR (300 MHz, DMSO-d_6) δ: 11.73 (s, 1H), 8.38 (s, 1H), 8.30 (d, J = 7.9 Hz, 1H), 7.90 (d, J = 8.7 Hz, 2H), 7.71–7.63 (m, 5H), 7.57 (t, J = 7.6 Hz, 1H), 7.27 (t, J = 7.2 Hz, 1H), 7.19 (d, J = 8.8 Hz, 2H), 3.91 (s, 3H), 3.81 (s, 4H), 3.02 (s, 4H), 1.29 (s, 9H); ^{13}C NMR (101 MHz, DMSO-d_6) δ: 167.6, 159.8, 156.4, 141.9, 141.4, 140.1, 132.8, 131.8, 130.0, 129.8, 129.5, 128.5, 127.6, 126.3, 121.8, 121.0, 120.0, 114.6, 114.2, 112.6, 55.4, 46.4, 41.4, 34.9, 30.7; MS (ESI): *m/z* 583 $[M+H]^+$; HRMS (ESI): *m/z* calcd for $C_{33}H_{35}N_4O_4S$: 583.23735; found: 583.23908 $[M+H]^+$.

4.2.16. (4-((4-Methoxyphenyl)sulfonyl)piperazin-1-yl)(1-(3,4,5-trimethoxyphenyl)-9*H*-pyrido[3,4-*b*]indol-3-yl)methanone (8da)

Cream colour solid:88% yield; mp: 157–159°C; ^{1}H NMR (300 MHz, DMSO-d_6) δ: 11.81 (s, 1H), 8.44 (s, 1H), 8.33 (d, J = 7.2 Hz, 1H), 7.65 (s, 3H), 7.57 (s, 1H), 7.28 (s, 1H), 7.17 (s, 2H), 7.10 (d, J = 27.4 Hz, 2H), 3.91 (s, 7H), 3.84 (s, 6H), 3.79 (s, 3H), 3.00 (s, 4H); ^{13}C NMR (101 MHz, DMSO-d_6) δ: 167.5, 162.9, 153.1, 141.8, 141.4, 140.2, 138.0, 133.1, 133.0, 129.7, 128.6, 126.2, 121.9, 121.0, 120.0, 115.2, 114.6, 112.6, 110.5, 105.8, 60.1, 55.8, 55.7, 46.3, 41.4; MS (ESI): *m/z* 617 $[M+H]^+$; HRMS (ESI): *m/z* calcd for $C_{32}H_{33}N_4O_7S$: 617.20645; found: 617.20909 $[M+H]^+$.

4.2.17. (4-Tosylpiperazin-1-yl)(1-(3,4,5-trimethoxyphenyl)-9*H*-pyrido[3,4-*b*]indol-3-yl)methanone (8db)

White solid:86% yield; mp: 145–147 °C;^{1}H NMR (300 MHz, DMSO-d_6) δ: 11.81 (s, 1H), 8.44 (s, 1H), 8.32 (d, J = 7.7 Hz, 1H), 7.62 (dd, J = 18.0, 9.1 Hz, 4H), 7.45 (d, J = 8.0 Hz, 2H), 7.34–7.21 (m, 1H), 7.11 (d, J = 35.5 Hz, 2H), 3.91 (s, 7H), 3.79 (s, 6H), 3.01 (s, 4H), 2.40 (s, 3H); ^{13}C NMR (101 MHz, DMSO-d_6) δ: 167.6, 153.1, 143.9, 141.8, 141.4, 140.2, 138.1, 133.1, 133.0, 131.9, 129.9, 129.6, 128.6, 127.5, 121.9, 121.0, 120.0, 115.3, 112.6, 105.8, 60.1, 55.8, 46.3, 41.4, 21.0; MS (ESI): *m/z* 601 $[M+H]^+$; HRMS (ESI): *m/z* calcd for $C_{32}H_{33}N_4O_6S$: 601.21153; found: 601.21387 $[M+H]^+$.

4.2.18. (4-((4-Chlorophenyl)sulfonyl)piperazin-1-yl)(1-(3,4,5-trimethoxyphenyl)-9*H*-pyrido[3,4-*b*]indol-3-yl)methanone (8dc)

White solid:84% yield; mp: 180–182°C;^{1}H NMR (300 MHz, DMSO-d_6) δ: 11.81 (s, 1H), 8.45 (s, 1H), 8.33 (d, J = 7.8 Hz, 1H), 7.74 (s, 4H), 7.71–7.62 (m, 2H), 7.59 (d, J = 7.5 Hz, 1H), 7.29 (t, J = 7.3 Hz, 1H), 7.18 (s, 1H), 3.87 (d, J = 20.3 Hz, 9H), 3.79 (s, 4H), 3.08 (d, J = 17.8 Hz, 4H); ^{13}C NMR (75 MHz, DMSO-d_6) δ: 167.5, 153.0, 141.8, 141.4, 140.1, 138.4, 138.0, 133.9, 133.0, 129.6, 129.3, 128.5, 121.9, 121.0, 120.0, 115.5, 115.2, 112.6, 105.8, 60.1, 55.8, 46.2, 41.4; MS (ESI): *m/z* 621 $[M+H]^+$; HRMS (ESI): *m/z* calcd for $C_{31}H_{30}ClN_4O_6S$: 621.15691; found: 621.15944 $[M+H]^+$.

4.2.19. (4-(Phenylsulfonyl)piperazin-1-yl)(1-(3,4,5-trimethoxyphenyl)-9*H*-pyrido[3,4-*b*]indol-3-yl)methanone (8dd)

Cream colour solid:85% yield; mp: 162–164°C;^{1}H NMR (300 MHz, DMSO-d_6) δ: 11.82 (s, 1H), 8.45 (d, J = 4.5 Hz, 1H), 8.32 (d, J = 7.9 Hz, 1H), 7.79–7.71 (m, 3H), 7.70 (d, J = 5.2 Hz, 1H), 7.68–7.61 (m, 3H), 7.57 (dd, J = 9.5, 5.5 Hz, 1H), 7.27 (dd, J = 13.4, 6.4 Hz, 1H), 7.18 (s, 1H), 3.91 (d, J = 4.2 Hz, 9H), 3.78 (s, 4H), 3.05 (d, J = 14.9 Hz, 4H); ^{13}C NMR (101 MHz, DMSO-d_6) δ: 167.6, 153.0, 141.7, 141.5, 140.1, 138.0, 134.8, 133.5, 133.2, 133.0, 129.5, 128.5, 127.4, 121.9, 121.0, 119.9, 115.2, 112.6, 110.5, 105.7, 60.1, 55.8, 46.3, 41.4; MS (ESI): *m/z* 587 $[M+H]^+$; HRMS (ESI): *m/z* calcd for $C_{31}H_{31}N_4O_6S$: 587.19588; found: 587.19804 $[M+H]^+$.

4.2.20. (4-((4-(Tert-butyl)phenyl)sulfonyl)piperazin-1-yl)(1-(3,4,5-trimethoxyphenyl)-9*H*-pyrido[3,4-*b*]indol-3-yl)methanone (8de)

White solid:86% yield; mp: 188–190°C;^{1}H NMR (300 MHz, DMSO-d_6) δ: 11.82 (s, 1H), 8.45 (s, 1H), 8.32 (d, J = 7.9 Hz, 1H), 7.66 (s, 4H), 7.59 (dd, J = 14.8, 7.2 Hz, 3H), 7.28 (t, J = 7.1 Hz, 1H), 7.16 (s, 1H), 3.87 (d, J = 19.9 Hz, 9H), 3.78 (s, 4H), 3.05 (s, 4H), 1.29 (s, 9H); ^{13}C NMR (101 MHz, DMSO-d_6) δ: 167.5, 156.4, 153.0, 141.7, 141.4, 140.2, 138.0, 134.0, 133.1, 132.0, 129.6, 128.5, 127.4, 126.3, 121.9, 121.0, 120.0, 115.3, 112.6, 105.8, 60.0, 55.8, 46.3, 41.4, 34.9, 30.7; MS (ESI): *m/z* 643 $[M+H]^+$; HRMS (ESI): *m/z* calcd for $C_{35}H_{39}N_4O_6S$: 643.25848; found: 643.26157 $[M+H]^+$.

4.2.21. (4-((4-Methoxyphenyl)sulfonyl)piperazin-1-yl)(1-phenyl-9*H*-pyrido[3,4-*b*]indol-3-yl)methanone (8ea)

Brown colour solid:85% yield; mp: >350°C;^{1}H NMR (400 MHz, DMSO-d_6) δ: 8.48 (s, 1H), 8.39 (d, J = 7.8 Hz, 1H), 7.67 (s, 2H), 7.65 (d, J = 2.4 Hz, 2H), 7.63 (d, J = 1.7 Hz, 2H), 7.59 (dd, J = 9.2, 3.3 Hz, 3H), 7.37–7.32 (m, 1H), 7.12 (d, J = 8.9 Hz, 2H), 3.83 (s, 3H), 3.75 (d, J = 19.6 Hz, 4H), 2.95 (s, 4H); ^{13}C NMR (75 MHz, DMSO-d_6) δ: 167.3, 162.8, 149.6, 142.7,

141.5, 138.8, 134.3, 129.7, 128.9, 128.5, 128.0, 125.9, 124.6, 121.9, 120.5, 120.3, 114.7, 114.5, 110.6, 55.6, 46.3, 41.3; MS (ESI): *m/z* 528 $[M+H]^+$; HRMS (ESI): *m/z* calcd for $C_{29}H_{27}N_4O_4S$: 527.17475; found: 527.17602 $[M+H]^+$.

4.2.22. (1-Phenyl-9*H*-pyrido[3,4-*b*]indol-3-yl)(4-tosylpiperazin-1-yl)methanone (8eb)

Brown colour solid:85% yield; mp: >350°C;^{1}H NMR (300 MHz, DMSO-d_6) δ: 8.48 (s, 1H), 8.39 (d, J = 7.8 Hz, 1H), 7.68 (s, 1H), 7.66 (d, J = 2.7 Hz, 2H), 7.62 (d, J = 2.0 Hz, 2H), 7.59 (d, J = 2.1 Hz, 3H), 7.57 (d, J = 2.5 Hz, 1H), 7.43 (d, J = 8.1 Hz, 2H), 7.38–7.30 (m, 1H), 3.75 (d, J = 14.0 Hz, 4H), 2.95 (s, 4H), 2.38 (s, 3H); ^{13}C NMR (75 MHz, DMSO-d_6) δ: 167.4, 156.8, 143.8, 142.7, 141.5, 138.8, 134.3, 131.6, 129.9, 129.7, 128.9, 128.5, 128.0, 127.5, 124.7, 121.9, 120.5, 120.3, 114.7, 110.6, 46.3, 41.3, 21.0; MS (ESI): *m/z* 512 $[M+H]^+$; HRMS (ESI): *m/z* calcd for $C_{29}H_{27}N_4O_3S$: 511.17984; found: 511.19204 $[M+H]^+$.

4.2.23. (4-((4-Chlorophenyl)sulfonyl)piperazin-1-yl)(1-phenyl-9*H*-pyrido[3,4-*b*]indol-3-yl)methanone (8ec)

Brown colour solid:82% yield; mp: >350°C;^{1}H NMR (300 MHz, DMSO-d_6) δ: 8.48 (s, 1H), 8.39 (d, J = 7.7 Hz, 1H), 7.75 (d, J = 8.0 Hz, 3H), 7.69 (d, J = 6.5 Hz, 4H), 7.60 (d, J = 11.4 Hz, 4H), 7.34 (s, 1H), 3.77 (s, 4H), 3.01 (s, 4H); ^{13}C NMR (101 MHz, DMSO-d_6) δ: 167.4, 142.7, 141.5, 138.8, 138.3, 134.3, 133.6, 129.8, 129.7, 129.6, 129.4, 129.3, 128.9, 128.5, 128.0, 121.9, 120.5, 120.3, 114.7, 110.6, 46.2, 41.3; MS (ESI): *m/z* 532 $[M+H]^+$; HRMS (ESI): *m/z* calcd for $C_{28}H_{24}ClN_4O_3S$: 531.12522; found: 531.12564 $[M+H]^+$.

4.2.24. (1-Phenyl-9*H*-pyrido[3,4-*b*]indol-3-yl)(4-(phenylsulfonyl)piperazin-1-yl)methanone (8ed):

Brown colour solid:80% yield; mp: 224–226°C;^{1}H NMR (500 MHz, DMSO-d_6) δ: 8.48 (s, 1H), 8.38 (d, J = 7.8 Hz, 1H), 7.75–7.72 (m, 2H), 7.72–7.68 (m, 2H), 7.67 (d, J = 8.7 Hz, 2H), 7.64 (d, J = 1.4 Hz, 1H), 7.63 (s, 2H), 7.62–7.59 (m, 1H), 7.58 (d, J = 6.7 Hz, 2H), 7.34 (t, J = 7.1 Hz, 1H), 3.76 (d, J = 20.7 Hz, 4H), 2.98 (s, 4H); ^{13}C NMR (101 MHz, DMSO-d_6) δ: 167.4, 142.7, 141.5, 138.8, 134.6, 134.3, 133.4, 129.9, 129.7, 129.4, 128.9, 128.5, 128.0, 127.5, 127.3, 121.9, 120.5, 120.3, 114.7, 110.6, 46.3, 41.3; MS (ESI): *m/z* 498 $[M+H]^+$; HRMS (ESI): *m/z* calcd for $C_{28}H_{25}N_4O_3S$: 497.16419; found: 497.16514 $[M+H]^+$.

4.2.25. (4-((4-(Tert-butyl)phenyl)sulfonyl)piperazin-1-yl)(1-phenyl-9*H*-pyrido[3,4-*b*]indol-3-yl)methanone (8ee)

Brown colour solid:88 % yield; mp: 197–199°C;[1]H NMR (300 MHz, DMSO-d_6) δ: 8.49 (s, 1H), 8.38 (d, J = 7.8 Hz, 1H), 7.68 (s, 2H), 7.64 (s, 5H), 7.62–7.55 (m, 4H), 7.34 (t, J = 6.2 Hz, 1H), 3.76 (d, J = 16.6 Hz, 4H), 2.99 (s, 4H), 1.28 (s, 9H); [13]C NMR (126 MHz, DMSO-d_6) δ: 167.4, 156.3, 142.7, 141.5, 138.8, 134.3, 131.7, 129.9, 129.7, 128.9, 128.5, 128.0, 127.5, 127.4, 126.2, 121.9, 120.5, 120.3, 114.7, 110.6, 46.3, 41.3, 34.9, 30.7; MS (ESI): *m/z* 554 $[M+H]^+$; HRMS (ESI): *m/z* calcd for $C_{32}H_{33}N_4O_3S$: 553.22679; found: 553.22720 $[M+H]^+$.

4.2.26. (4-((4-Methoxyphenyl)sulfonyl)piperazin-1-yl)(9*H*-pyrido[3,4-*b*]indol-3-yl)methanone (8fa)

Cream colour solid:90% yield; mp: 195–197°C;[1]H NMR (300 MHz, DMSO-d_6) δ: 11.88 (s, 1H), 8.82 (s, 1H), 8.42 (s, 1H), 8.29 (d, J = 7.9 Hz, 1H), 7.69 (d, J = 8.8 Hz, 2H), 7.60 (dd, J = 13.6, 7.4 Hz, 2H), 7.26 (t, J = 6.9 Hz, 1H), 7.18 (d, J = 8.9 Hz, 2H), 3.86 (s, 3H), 3.76 (s, 4H), 3.02–2.84 (m, 4H); [13]C NMR (101 MHz, DMSO-d_6) δ: 167.7, 162.9, 142.0, 140.9, 136.0, 131.9, 129.8, 128.6, 127.9, 126.0, 122.1, 120.6, 119.8, 116.0, 114.6, 112.1, 55.7, 46.1, 41.2; MS (ESI): *m/z* 451 $[M+H]^+$; HRMS (ESI): *m/z* calcd for $C_{23}H_{23}N_4O_4S$: 451.14345; found: 451.14372 $[M+H]^+$.

4.2.27. (9*H*-Pyrido[3,4-*b*]indol-3-yl)(4-tosylpiperazin-1-yl)methanone (8fb)

White solid:88% yield; mp: 162–164°C;[1]H NMR (300 MHz, DMSO-d_6) δ: 8.82 (s, 1H), 8.42 (d, J = 0.8 Hz, 1H), 8.29 (d, J = 7.9 Hz, 1H), 7.63 (t, J = 6.4 Hz, 3H), 7.60–7.53 (m, 1H), 7.47 (d, J = 8.1 Hz, 2H), 7.26 (t, J = 7.3 Hz, 1H), 3.75 (s, 4H), 2.94 (d, J = 26.9 Hz, 4H), 2.42 (s, 3H); [13]C NMR (75 MHz, DMSO-d_6) δ: 167.7, 143.8, 141.9, 140.9, 136.0, 131.9, 131.7, 129.9, 128.5, 127.9, 127.6, 122.0, 120.6, 119.7, 116.0, 112.1, 46.1, 41.2, 21.0; MS (ESI): *m/z* 435 $[M+H]^+$; HRMS (ESI): *m/z* calcd for $C_{23}H_{23}N_4O_3S$: 435.14854; found: 435.14900 $[M+H]^+$.

4.2.28. (4-((4-Chlorophenyl)sulfonyl)piperazin-1-yl)(9*H*-pyrido[3,4-*b*]indol-3-yl)methanone (8fc)

Cream colour solid: 86% yield; mp: 160–162°C; [1]H NMR (300 MHz, DMSO-d_6) δ: 8.83 (s, 1H), 8.42 (s, 1H), 8.29 (d, J = 7.9 Hz, 1H), 7.76 (d, J = 2.7 Hz, 3H), 7.70 (s, 1H), 7.66–7.52 (m, 2H), 7.33–7.20 (m, 1H), 3.76 (s, 4H), 2.98 (d, J = 17.2 Hz, 4H); [13]C NMR (101 MHz, DMSO-d_6) δ: 167.8, 141.9, 140.9, 138.4, 136.0, 133.7, 131.9, 129.7, 129.5, 128.5, 127.9,

122.1, 120.6, 119.8, 116.1, 112.2, 46.2, 41.2; MS (ESI): *m/z* 455 $[M+H]^+$; HRMS (ESI): *m/z* calcd for $C_{22}H_{20}ClN_4O_3S$: 455.09392; found: 455.09469 $[M+H]^+$.

4.2.29. (4-(Phenylsulfonyl)piperazin-1-yl)(9*H*-pyrido[3,4-*b*]indol-3-yl)methanone (8fd)

Cream colour solid:84% yield; mp: 236–238°C; ^{1}H NMR (300 MHz, DMSO-d_6) δ: 11.88 (s, 1H), 8.82 (s, 1H), 8.42 (s, 1H), 8.29 (d, J = 7.9 Hz, 1H), 7.80–7.72 (m, 3H), 7.69 (d, J = 7.1 Hz, 2H), 7.66–7.60 (m, 1H), 7.60–7.53 (m, 1H), 7.26 (t, J = 7.3 Hz, 1H), 3.76 (s, 4H), 2.97 (t, J = 13.7 Hz, 4H); ^{13}C NMR (101 MHz, DMSO-d_6) δ: 167.8, 141.9, 140.9, 136.0, 134.6, 133.4, 131.9, 129.5, 128.6, 127.9, 127.5, 122.1, 120.6, 119.8, 116.1, 112.2, 46.3, 41.2; MS (ESI): *m/z* 421 $[M+H]^+$; HRMS (ESI): *m/z* calcd for $C_{22}H_{21}N_4O_3S$: 421.13289; found: 421.13339 $[M+H]^+$.

4.2.30. (4-((4-(Tert-butyl)phenyl)sulfonyl)piperazin-1-yl)(9*H*-pyrido[3,4-*b*]indol-3-yl)methanone (8fe)

White solid:86 % yield; mp: 282–284°C; ^{1}H NMR (300 MHz, DMSO-d_6) δ: 11.88 (s, 1H), 8.82 (s, 1H), 8.43 (s, 1H), 8.29 (d, J = 7.8 Hz, 1H), 7.69 (s, 4H), 7.66–7.50 (m, 2H), 7.26 (t, J = 7.3 Hz, 1H), 3.76 (s, 4H), 2.96 (d, J = 27.7 Hz, 4H), 1.32 (s, 9H); ^{13}C NMR (101 MHz, DMSO-d_6) δ: 167.8, 156.4, 141.9, 140.9, 136.0, 131.9, 128.6, 127.9, 127.5, 126.3, 122.1, 120.6, 119.8, 116.1, 112.2, 46.2, 41.2, 34.9, 30.7; MS (ESI): *m/z* 477 $[M+H]^+$; HRMS (ESI): *m/z* calcd for $C_{26}H_{29}N_4O_3S$: 477.19549; found: 477.19595 $[M+H]^+$.

4.3. Biology

4.3.1. Cytotoxic assay

The cytotoxic activity of the **8aa-fe** was determined using MTT assay. Briefly, cells were plated at a density of 5×10^3 cells/well were seeded, supplemented with 10% FBS in each well of 96-well microculture plates and incubated for 24 h at 37^{o}C in 5% CO_2 incubator. After 24 h of incubation, all the synthesized derivatives were added to the cells and incubated for 48 h. After 48 h of drug treatment, cell viability was determined by adding 100µL/well of MTT reagent (0.5 mg/mL) to each well and the plates were further incubated for 4 h. Then the supernatant from each well was carefully removed, the formazon crystals were dissolved in 200µL of DMSO and absorbance was measured at 570 nm using multimode plate reader (BioTek Instruments, Synergy 4, and Winooski, VT).

4.3.2. DNA topo II inhibition assay

In order to determine the effect of **8ec** and **8ed** in topoisomerase II inhibition and the formation efficiency of decatenated kDNA was studied using the protocol mentioned in topoisomerase II Drug Screening Kit (TG 1009, Topogen, USA). Topoisomerase II inhibition was assayed using the ATP dependent decatenation of kDNA and all the reactions were carried out in 20 mL and contained 120mM KCl, 50mM Tris-HCl, pH 8, 10mM $MgCl_2$, 0.5mM dithiothreitol, 0.5 mM ATP, 30 mg/mL bovine serum albumin, 200-300 ng of kDNA, and topoisomerase II. The amount of topoisomerase II (5 units) was adjusted in preliminary experiments to decatenate approximately 100% of the kDNA under these assay conditions. The reactions samples were incubated at 37 ^oC for 30 min and terminated by the addition of 2 mL of a stop buffer containing 10% (w/v) SDS and 2 ml of 0.5 mg/mL proteinase-K and incubated for 10 min at 37 ^oC. After completion of the reaction, the products in the reaction mixture were separated by 1% agarose gel and visualized after staining with ethidium bromide (0.2l g/mL). The gels were run at 100 V for about 40 min and visualized under UV transillumination (BIO RAD gel doc XR^+, USA).

4.3.3. Apoptotic induction studies

4.3.3.1. Cell cycle Analysis

Flow cytometric analysis (FACS) was performed to calculate the distribution of the cell population through the cell cycle phases.MG-63 cells were incubated with compounds**8ed** (0.5 μM) and **8ec** (2 μM) for 24 h. Untreated and treated cells were harvested, washed with PBS, fixed in ice-cold 70%ethanol and stained with propidium iodide reagent (50 μg/mL), in the presence of Rnase A containing 0.1% Triton X-100for 30 min at 37 ^oC in dark, and about 10,000 events were analyzed by flow cytometer BD FACSVerseTM, USA.

4.3.3.2. Phase contrast Microscopy

MG-63 cells were seeded at a density of $1x10^6$cells/mL in 6 well plates and incubated overnight. The cells were incubated with the **8ed** (0.5 μM) and **8ec** (2 μM). After 48 h treatment, morphological changes were observed in the cells and images were captured under a phase contrast microscope (Nikon, Inc. Japan).

4.3.3.3. Acridine orange/ethidium bromide (AO/EB) staining

MG-63 cells were plated at a concentration of $1x10^6$cells/mL and treated with **8ed** (0.5 μM) and **8ec** (2μM). Plates were incubated for 48 h at 37 ^oC. 10 μL each from 1mg/mL stock solution of fluorescent dyes containing AO/EB were added into each well in equal volumes

(10 μg/mL) respectively. Cells were visualized under fluorescence microscope (Nikon, Inc. Japan) with excitation (488 nm) and emission (550 nm) at 200X magnification.

4.3.3.4. DAPI staining

Nuclear morphological changes were observed through DAPI staining. After treatment with compounds **8ed** (0.5 μM) and **8ec** (2μM) for 48 h, MG-63 cells were washed with PBS and permeabilized with 0.1% Tween 20 for 10 min followed by staining with DAPI. Control and treated cells were observed with fluorescence microscope with excitation at 359 nm and emission at 461 nm using DAPI filter at 200X magnification.

4.3.3.5. DCFDA staining

In this assay, MG-63 cells were seeded at a density of 0.7×10^5 cells/well into 12-well plates in RPMI supplemented with 10% FBS. Cells were treated with the compounds **8ed** (0.5 μM) and **8ec** (2μM) for 24 h. Then the DCFDA reagent was added at 10 μM concentration for 15 min. Cells were then washed three times with PBS to remove the excess dye and the fluorescent intensity was captured using fluorescent microscope at 200X magnification.

4.3.3.6. Effect of 8ed and 8ec on mitochondrial membrane potential (ΔΨm)

MG-63 cells were seeded at a density of 0.7×10^5cells/well in 12-well plates and allowed to adhere for overnight. Cells were incubated with compounds **8ed** (0.5 μM) and **8ec** (2μM) for 48 h. Cells were collected, washed with PBS and resuspended in JC-1 dye (1μM) and incubated for 30 min in incubator at 37 ^{o}C. The cells were washed twice with PBS and cells were trypsinized, centrifuged and analyzed by flow cytometry (BD FACSVerseTM, USA).

4.3.3.7. Annexin V/Dead Cell Apoptosis assay

MG-63 cells were seeded at a density of $0.7x10^5$ cells/well in 12 well plate and treated with compounds **8ed** (0.5 μM) and **8ec** (2μM) for 48 h. Then the cells were processed with Alexa Fluor® 488 annexin V/Dead Cell Apoptosis Kit, (Thermo Fisher Scientific USA) according to the manufacturer's instructions. Further, samples were analyzed by flow cytometry.

4.3.4. DNA binding studies

4.3.4.1. UV-visible spectroscopy.

UV-visible absorption spectra were recorded using Perkin Elmer ABI 35 Lambda Spectrophotometer (Waltham, MA, USA) at 25 ^{o}C. All the titrations were carried out in polystyrene cuvettes to minimize binding of compounds to the surface of the cuvettes. Then, 50 μM of **8ec** and **8ed** stock solution was prepared in DMSO and 25.0 μM of CT-DNA in 100 mM Tris-HCl (pH 7.0). About 1 mL of 25.0 μM conjugate solution was taken in a 1 cm

path length cuvette and 5 mL of DNA was added to each titration. All the stock solutions used were freshly prepared before commencing the experiment, titration was carried out until saturation of absorbance occurs and the absorption spectra recorded in the range of 200 nm to 400 nm.

4.3.4.2. Fluorescence spectroscopy

Fluorescence emission spectra were measured at 25 ^{o}C using a Hitachi F7000 spectrofluorimeter (Maryland, USA) using a 1 cm path length quartz cuvette. Initially, quartz cuvettes was thoroughly washed with distilled water and dilute nitric acid (approximately 0.1 N) to minimize non-specific binding of the compounds to the surface of the cuvette. Throughout the fluorescence experiment, concentration of **8ec** and **8ed** were kept constant (10 μM) and titrated with equally increasing concentrations of CT-DNA (multiples of 0.5 μM). Fluorescence spectra were recorded after each addition of CT-DNA to the fluorescent cuvette. The compounds were excited at 230 nm and emission spectrum for each titration was recorded at their maximum emission wavelength. The average of three scans was taken after recording three individual spectrum.

4.3.4.3. Circular dichorism (CD) studies.

DNA conformational studies were carried out on a JASCO 815 CD spectropolarimeter (Jasco, Tokyo, Japan). CD Spectroscopic studies were performed to study the change in DNA conformation brought by **8ec** and **8ed**compoundson interaction with CT-DNA at micro molar concentration range. The CT-DNA solution was prepared in 100 mM Tris-HCl (pH 7.0) and 10 μM of CT-DNA added about 10.0 μM and 20 μM (1:1 and 1:2 ratio of DNA:conjugate) of each solution containing **8ec** and **8ed** conjugatewas added and CD spectra was recorded from 200 nm to 350 nm using 1mmpath length cuvette. The spectra were averaged over 3 scans.

4.3.4.4. Viscosity studies

Viscosity experiments were conducted on Ostwald viscometer, immersed in a water bath maintained at 25 ^{o}C. Viscosity experiments were performed for each conjugate (15 mM), after mixing them with CT-DNA solution (150 μM). Before mixing DNA and compounds, viscosity measurements were performed with CT-DNA alone. Et Br-CT-DNA and Hoechst 33342-CT-DNA complexes were considered as control. DNA solution was prepared in 100 mM Tris-HCl (pH 7.0). Graph was drawn by plotting $(\eta/\eta_o)^{1/3}$ versus complex/ CT-DNA, where η is the viscosity of CT-DNA in the presence of β-carboline linked sulphonamide compounds and η_o is the viscosity of CT-DNA alone.

Acknowledgements

The authors thank and acknowledge the Department of Pharmaceuticals, Ministry of Chemicals & Fertilizers and Indian Institute of Chemical Technology (CSIR-IICT), Hyderabad for providing funds, Scientific and Instrumental support.

References

[1] (a) https://www.cancer.gov/about-cancer/understanding/statistics; (b) http://www.who.int/mediacentre/factsheets/fs297/en

[2] R. Siegel, K. D. Miller, A. Jemal, CA, Cancer J. Clin. 67(2017) 7-30.

[3] (a) L. H. Hurley, Nat. Rev. Cancer. 2 (2002) 188-200; (b) J. Sheng, J. Gan, Z. Huang, Med Res Rev. 33 (2013) 1119-1173; (c) S. Nekkanti, R. Tokala, N. Shankaraiah, Curr. Med. Chem. 24 (2017) 2887-2907.

[4] (a) E.J. Massaro, Handbook of Neurotoxicology, Humana Press, (2002) 237; (b) N. Devi, S. Kumar, S.K. Pandey, V. Singh, Asian J. Org. Chem.(2017) 6-36.

[5] (a) R. Cao, W. Peng, Z. Wang, A. Xu, Curr. Med. Chem. 14 (2007) 479-500; (b)Y. Wang, J. Shao, S. Yao, S. Zhang, J. Yan, H. Wang, Y. Chen, Carbohydr. Polym. 105 (2014) 231-236; (c) K. Yao, M. Zhao, X. Zhang, Y. Wang, L. Li, M. Zheng, S. Peng, Eur. J. Med. Chem. 46 (2011) 3237-3249; (d) R. B. Volk and F. H. Furkert, Microbiol. Res.161 (2006) 180-186; (e) R. Frederick, C. Bruyere, C. Vancraeynest, J. Reniers, C. Meinguet, L. Pochet, A. Backlund, B. Masereel, R. Kiss and J. Wouters, J. Med. Chem.55 (2012) 6489-6501; (f) Y. Rook, K. U. Schmidtke, F. Gaube, D. Schepmann, B. Wunsch, J. Heilmann, J. Lehmann and T. Winckler, J. Med. Chem. 53 (2010) 3611-3617; (g) R. Brokamp, B. Bergmann, I.B. Müller, S. Bienz, Bioorg. Med. Chem. 22 (2014) 1832-1837; (h) W. Polanski, H. Reichmann and G. Gille, Expert. Rev. Neurother.11 (2011) 845-860.

[6] (a) S. Xiao, W. Lin, C. Wang, M. Yang, Bioorg. Med. Chem. Lett. 11 (2001) 437-441; (b) K. Hayashi, M. Nagao, T. Sugimura, Nucleic Acids Res. 4 (1977) 3679-3685.

[7] (a) A.M. Deveau, M.A. Labroli, C.M. Dieckhaus, M.T. Barthen, K.S. Smith, T.L. Macdonald, Bioorg. Med. Chem. Lett. 11 (2001) 1251-1255; (b) M. Zhao, L. Bi, W. Wang, C. Wang, Bioorg. Med. Chem. 14 (2006) 6998-7010; (c) R. Chaniyara, S. Tala, C.W. Chen, X. Zang, R. Kakadiya, L.F. Lin, C.H. Chen, S.I. Chien, T.C. Chou, T.H. Tsai, T.C. Lee, A. Shah, T.L. Su, J. Med. Chem. 56 (2013) 1544-1563.

[8] P. A. Barsanti, W. Wang, Z. Ni, D. Duhl, N. Brammeier and E. Martin, Bioorg. Med. Chem. Lett. 20 (2010) 157–160.

[9] (a) A. C. Castro, L. C. Dang, F. Soucy, L. Grenier, H. Mazdiyasni, M. Hottelet, L. Parent, C. Pien, V. Palombella and J. Adams, Bioorg. Med. Chem. Lett.13 (2003) 2419–2422. (b) J. I. Trujillo, M. J. Meyers, D. R. Anderson, S. Hegde, M. W. Mahoney, W. F. Vernier, I. P. Buchler, K. K. Wu, S. Yang, S. J. Hartmann and D. B. Reitz, Bioorg. Med. Chem.Lett.17 (2007) 4657–4663.

[10] Y. Song, J. Wang, S.F. Teng, D. Kesuma, Y. Deng, J. Duan, J.H. Wang, R.Z. Qi, M.M. Sim, Bioorg. Med. Chem. Lett. 12 (2002) 1129-1132.

[11] S. Li, A. Wang, F. Gu, Z. Wang, C. Tian, Z. Qian, L. Tang, Y. Gu, Oncotarget. 6 (2015) 8988-9001.

[12] Z. Chen, R. Cao, B. Shi, W. Yi, L. Yu, H. Song, Z. Ren, W. Peng, Bioorg. Med. Chem. Lett. 20 (2010) 3876-3879.

[13] L. C. Tu, C. S. Chen, I. C. Hsiao, J. W. Chern, C. H. Lin, Y. C. Shen, S.F. Yeh, Chem. Biol. 12 (2005) 1317-1324.

[14] A. Kamal, M.N. Rao, P. Swapna, V. Srinivasulu, C. Bagul, A.B. Shaik, K. Mullagiri, J. Kovvuri, V.S. Reddy, K. Vidyasagar, Org. Biomol. Chem. 12 (2014) 2370-2387.

[15] R. J. Man, D. J. Tang, X. Y. Lu, Y. T. Duan, X. X. Tao, M. R. Yang, L. L. Wang, B. Z. Wang,C. Xuand H. L. Zhu, Med. Chem.commun. 7 (2016) 1759–1767.

[16] S. M. Kupchan, R. W. Britton, M. F. Ziegler, C. J. Gilmore, R. J. Restivo and R. F. Bryan, J. Am. Chem. Soc.95 (1973) 1335–1336; P. K. Naik, B. P. Chatterji, S. N. Vangapandu, R. Aneja, R. Chandra and S. Kanteveri, J. Comput. Aided Mol. Des. 25 (2011) 443–454.

[17] S. M. Attia, J. Appl. Toxicol. 10 (2011)1002–1753

[18] R. J. Kerns, M. J. Rybak, G. W. Kaatz, F. Vaka, R. Cha, R. G. Grucz and V. U. Diwadkar, Bioorg. Med. Chem. Lett.13 (2003) 2109–2112.

[19] C. Avijeet, A. Amy and G. Charles, J. Biol. Chem.289 (2014) 2978–2991.

[20] A. Nagarsenkar, S. K. Prajapti, S. D. Guggilapu, S. Birineni, S. S. Kotapalli, R. Ummanni, B. N. Babu, Med. Chem. Commun. 7 (2016) 646-653.

[21] C. V. Junior, A. Danuello, V. da Silva Bolzani, E. J. Barreiro, C. A. Fraga, Curr. Med. Chem. 14 (2007)1829-1852.

[22] J. L. Nitiss, W.T. Beck, Eur. J. Cancer.6 (1996), 958 –966.

[23] Y. Pommier, E. Leo, H. L. Zhang, Chemistry & Biology.17 (2010) 421–433.

[24] A.D. Bates, A. Maxwell, Biochemistry. 46 (2007) 7929–7941.

[25] N. P. Kumar, S. Thatikonda, R. Tokala, S.S.Kumari, U.J.Lakshmi,C. Godugu, N. Shankaraiah, A. Kamal,Bioorg. Med. Chem. 26 (2018) 1996-2008.

[26] V. Pooladanda, S. Thatikonda, S. Bale, B. Pattnaik,D.K. Sigalapalli, N.B. Bathini, S. B. Singh, C. Godugu, Cell death & disease. 28 (2019) 81.

[27] J. Wu, M. Zhao, K. Qian, K. H. Lee, S. M. Natschke, S. Peng, Eur. J. Med.Chem. 44 (2009) 4153-4161.

[28] N. Shahabadi, S. Kashanian and M. Purfoulad, Spectrochim. Acta. 72 (2009) 757-761.

[29] J. M. Kelly, A. B. Tossi, D. J. Mcconnell and C. Ohui-gin, Nucleic Acids Res.13 (1985) 6017–6034.

[30] C. Metcalfe, C. Rajput and J. A. Thomas, J. Inorg. Biochem. 100 (2006)1314-1319.

[31] H. Wei, A. J. Ruthenburg, S. K. Bechis, G. L.Verdine, J. Biol. Chem. 280 (2005) 37041-37047.

[32] Schrödinger Suite 2017-1, Schrödinger, LLC, New York, (2017).

[33] M. K. Teng, N. Usman, C. A. Frederick, A. H. Wang, Nucleic Acids Res. 16 (1988) 2671-2690.

Research Highlights

- A series of *β*-carboline linked aryl sulfonyl piperazine conjugates (**8aa-fe**) were synthesized and screened for their anti-proliferative activity.
- Compounds **8ec** and **8ed** showed significant cytotoxicity with IC_{50} values 2.80±0.10 μM and 0.59±0.28 μM on MG-63 cell line.
- **8ec and 8ed arrest the cell cycle at sub G1 phase/ G2 phase and also assayed for DNA topo II inhibition study.**
- DNA binding studies and molecular docking studies revealed that **8ec** and **8ed** conjugates interact with DNA and they may bind to the surface of CT DNA.

Design and Synthesis of β-carboline linked aryl sulfonyl piperazine derivatives: DNA topoisomerase II inhibition with DNA binding and apoptosis inducing ability

Kesari Lakshmi Manasa,[a,b] Sowjanya Thatikonda,[c] Dilep Kumar Sigalapalli,[a,b] Arpita Sagar,[e] Gaddam Kiranmai,[d] Arunasree M Kalle,[e] Mallika Alvala,[b] Chandraiah Godugu,[c]* Narayana Nagesh,[d]* and Bathini Nagendra Babu[a]*

[a]*Fluoro-Agrochemicals, CSIR-Indian Institute of Chemical Technology, Hyderabad-500 007, India*

[b]*Department of Medicinal Chemistry, National Institute of Pharmaceutical Education and Research (NIPER), Hyderabad-500 037, India*

[c]*Department of Regulatory Toxicology, National Institute of Pharmaceutical Education and Research (NIPER), Hyderabad-500 037, India*

[d]*CSIR-Centre for Cellular and Molecular Biology, Hyderabad 500 007, India*

[e]*Department of Animal Biology, School of Life Sciences, University of Hyderabad, Hyderabad-500 046, India*

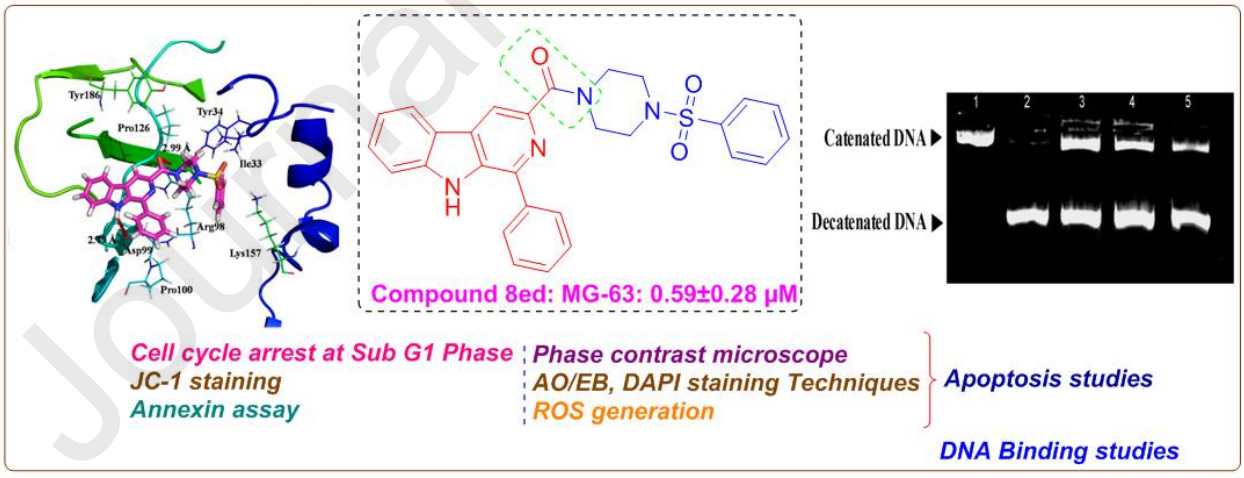

Conflicts of Interest

There is no conflicts of Interest.